

# **DESIGN, CONTROL AND SIMULATION OF PMSG BASED STAND-ALONE WIND ENERGY CONVERSION SYSTEM**

A thesis submitted in partial fulfilment  
Of the requirements for the award of the degree of

**Dual Degree [B.Tech/M.Tech]**

In

**Electrical Engineering**

**Submitted By**

Debabrata Thatoi

Roll no-710ee2034

**Under the guidance of**

Prof. Monalisha Pattnaik



Department of Electrical Engineering  
National Institute of Technology, Rourkela,  
Odisha-769008



**Department of Electrical Engineering**  
**National institute of Technology, Rourkela**

## **CERTIFICATE**

*This is to certify that the thesis entitled “**DESIGN, CONTROL AND SIMULATION OF PMSG BASED STAND-ALONE WIND ENERGY CONVERSION SYSTEM**” being submitted by Mr. Debabrata Thatoi to National Institute of Technology, Rourkela (Deemed University) for the award of Dual degree in Electrical Engineering Department with specialization in “**power electronics and drive**”, is a bonafide research work carried out by him in the **Department of electrical engineering**, under my supervision and guidance. I believe that this thesis fulfills the part of the requirement for the award of degree of Master of technology. The research reports and the results embodied in this thesis have not been submitted in parts or full to any other university or institution for the award of any other degree or diploma*

**Prof Monalisha Pattnaik**

Dept. of Electrical Engineering

National Institute of Technology

Rourkela, Odisha, 769008

INDIA

Place : N.I.T Rourkela

Date : 28/05/2015

## ACKNOWLEDGEMENT

*First and foremost, I am truly indebted and wish to express my gratitude to my supervisor Professor Monalisha Pattnaik for her inspiration, excellent guidance, continuing encouragement and unwavering confidence and support during every stage of this endeavor without which, it would not have been possible for me to complete this undertaking successfully. I also thank her for his insightful comments and suggestions which continually helped me to improve my understanding. I express my deep gratitude to the members of Masters Scrutiny Committee,*

*I am also very much obliged to the Head of the Department of Electrical Engineering, NIT Rourkela for providing all possible facilities towards this work. Thanks to all other faculty members in the department.*

*I would also like to express my heartfelt gratitude to my friends who have always inspired me and particularly helped me in my work.*

*My whole hearted gratitude to my parents for their constant encouragement, love, wishes and support. Above all, I thank Almighty who bestowed his blessings upon us.*

Debabrata Thatoi

Rourkela, May 2015

# ABSTRACT

In last decade, due to several limitations of conventional sources of energy such as high cost of fossil fuels, contribution towards pollution and environmental damage, scarcity in resources, there is an urge for the utilization of renewable sources of energy. Among several forms of renewable sources of energy, specifically wind energy conversion system is the most cost effective and technologically improvable. In variable speed operation, it is important that the generated power from PMSG should be optimized. Therefore in order to capture as much power as possible from wind during change in wind speed, maximum power point tracking controller is implemented. Among several methods, the most efficient method of MPPT technique is Perturbation and observation (P&O) which has its own virtues. Here simulation evaluation is done to know the working of MPPT and successfully optimize the generated power during a step change in wind speed. In addition to power optimization, variation in load as well as wind speed during variable speed operation, results drift in system voltage and frequency which in turn leads to generation loss owing to line tripping, power swings and also black outs. Therefore in order to reduce the change in system voltage and frequency to the smallest possible value, a voltage frequency controller is required. Therefore the simulation of WECS with a voltage frequency control using a VSC and BESS is performed. The Voltage frequency controller receives/supplies active/reactive power and hence system voltage and system frequency is maintained almost constant around its reference value. For this three phase three wire systems is considered. The performance of the system is also evaluated for change in load and fault occurrence at line. A PMSG based stand-alone WECS with VF controller is designed, modeled and simulated with MATLAB & SIMULINK.

# CONTENTS

CERTIFICATE .....	i
ACKNOWLEDGEMENT.....	ii
ABSTRACT .....	iii
List of figures .....	vi
List of tables .....	viii
List of symbols .....	ix
CHAPTER 1 .....	1
1.1    INTRODUCTION .....	1
1.2    LITERATURE REVIEW .....	2
1.3    MOTIVATION.....	3
1.4    OBJECTIVE .....	4
1.5    STRUCTURE OF THESIS .....	6
CHAPTER 2.....	8
2.1    DYNAMICS OF DIFFERENT COMPONENTS OF PMSG BASED SWECS.....	8
2.1.1    Wind turbine characteristics.....	8
2.1.2    Two mass drive train.....	10
2.1.3    Permanent magnet synchronous generator (PMSG).....	11
2.1.4    AC to DC three phase diode rectifier.....	13
2.1.5    Boost Converter .....	14
2.1.6    MPPT Controller.....	15
2.2    SIMULATION OF PMSG BASED SWECS WITH MPPT CONTROL .....	21
2.2.1    Two mass drive train.....	21
2.2.2    Wind turbine, two mass drive train and PMSG .....	22
2.2.3    Boost converter .....	23
2.3    SIMULATION RESULTS .....	25
CHAPTER 3.....	28
3.1    OVERVIEW ON VOLTAGE FREQUENCY CONTROLLER.....	28
3.1.1    Types of voltage frequency control schemes .....	29
3.1.2    Implementation of a Voltage Frequency controller using a VSC and BESS.....	30

3.2	DYNAMICS OF VOLTAGE FREQUENCY (VF) CONTROLLER, VSC AND BESS.....	30
3.2.1	Voltage Frequency Controller (VFC) .....	30
3.2.2	PWM generator .....	33
3.2.3	Voltage Source Converter (VSC) .....	33
3.2.4	Battery Energy Storage System (BESS) .....	34
3.3	SIMULATION OF VF CONTROLLER, VSC AND BESS.....	34
3.3.1	Battery energy storage system (BESS) .....	34
3.3.2.	Voltage source converter (VSC) .....	35
3.3.3	Voltage frequency controller (VFC) .....	35
3.3.4	Three phase three wire loads.....	36
3.3.5	Interfacing inductors .....	37
3.3.6	Maximum current through IGBT .....	37
3.4.1	Simulation result for variable wind speed.....	39
3.4.2	Simulation result for load change .....	45
3.4.3	Simulation for Fault current occurrence at line .....	50
CHAPTER 4.....		53
CONCLUSION.....		53
SCOPE OF FUTURE WORK .....		54
REFERENCE .....		55

## List of figures

Sl. No.	Details of Figures	Page No.
Fig 2.1	Circuit diagram of Permanent Magnet Synchronous Generator .....	13
Fig 2.2	Circuit diagram of a boost converter.....	14
Fig 2.3	Block diagram for optimal torque control.....	15
Fig 2.4	Block diagram for PSF MPPT control .....	16
Fig 2.5	Plot of power coefficient Vs tip speed ratio.....	17
Fig 2.6	Block diagram for Tip speed ratio MPPT control.....	17
Fig 2.7	Plot of generated power Vs. Generator speed.....	18
Fig 2.8	Plot of dc link power vs dc link voltage.....	19
Fig 2.9	Flow chart for P&O MPPT control.....	20
Fig 2.10	Circuit diagram for boost converter with MPPT controller .....	21
Fig 2.11	Simulink model diagram for two mass drive train.....	22
Fig 2.12	Simulink model for wind turbine, two mass drive train and PMSG.....	22
Fig 2.13	Simulink diagram for Boost converter.....	23
Fig 2.14	Simulink model of SWECS with MPPT control .....	24
Fig 2.15	Variable wind speed.....	25
Fig 2.16	Output generated power of PMSG.....	26
Fig 2.17	Dc link voltage of boost converter .....	26
Fig 2.18	Rotor speed of PMSG .....	27
Fig 3.1	Circuit diagram for VF controller using VSC and BESS.....	28
Fig 3.2	Block diagram of SRF technique of VF control .....	32
Fig 3.3	PWM generator .....	33
Fig 3.4	Circuit diagram of VSC .....	33
Fig 3.5	Circuit diagram of Battery energy storage system.....	34
Fig 3.6	Simulink model for SRF scheme based VF control.....	36
Fig 3.7	Simulink model for three phase three wire loads and three phase fault .....	36
Fig 3.8	Ripple filter .....	37
Fig 3.9	Simulink model of SWECS with VF controller.....	38

Fig 3.10	Variable wind speed.....	39
Fig 3.11	Three phase generated voltage of PMSG.....	39
Fig 3.12	Terminal voltage of PMSG .....	40
Fig 3.13	System frequency .....	40
Fig 3.14	Load current .....	41
Fig 3.15	Power produced by wind turbine .....	41
Fig 3.16	Generated power of PMSG .....	42
Fig 3.17	Load power .....	42
Fig 3.18	Battery power .....	43
Fig 3.19	Battery terminal voltage.....	43
Fig 3.20	Rotor speed of PMSG .....	44
Fig 3.21	IGBT current .....	44
Fig 3.22	Generated three phase ac voltage of PMSG.....	45
Fig 3.23	RMS voltage of three phase ac generated voltage. ....	45
Fig 3.24	Rotor speed of PMSG .....	46
Fig 3.25	Terminal voltage of PMSG .....	46
Fig 3.26	System frequency .....	47
Fig 3.27	Generated power of PMSG .....	47
Fig 3.28	Load power .....	48
Fig 3.29	Battery power .....	48
Fig 3.30	Battery terminal voltage.....	49
Fig 3.31	Load current .....	49
Fig 3.32	Three phase ac generated voltage of PMSG .....	50
Fig 3.33	Terminal voltage of PMSG .....	50
Fig 3.34	System frequency .....	51
Fig 3.35	Total generated power of PMSG .....	51
Fig 3.36	Battery power .....	52
Fig 3.37	Battery terminal voltage.....	52



## List of tables

Sl. No.	Details of Tables	Pages No
Table 2.1	PMSG parameters for simulation.....	22
Table 2.2	Wind turbine parameters.....	22
Table 2.3	Boost converter parameters.....	23

## List of symbols

$P$	Power in the wind stream
$C_p$	Power coefficient
$P_{Total}$	Total power received by wind turbine at intersection
$\lambda$	Tip speed ratio
$\beta$	Pitch angle
$F$	Thrust force
$T$	Rotor torque
$R$	Radius of the wind turbine blade
$C_T$	Torque coefficient
$T_{Total}$	Total torque received by the wind turbine at the intersection
$N$	Rotor speed in rpm
$H$	Inertia constant of machine
$\omega_t$	Speed of wind turbine in
$T_m$	Mechanical torque
$T_s$	Shaft torque
$\omega_{ebs}$	Electrical base speed
$\theta_{sta}$	Shaft twist angle
$\omega_r$	Rotor speed
$K_{ss}$	Shaft stiffness
$D_t$	Damping coefficient
$f$	Frequency of the system
$p$	No of poles
$\phi_f$	Air flux

$F_f$	MMF produced by flux
$e_{af}$	Voltage induced in the coil
$E_f$	RMS value of the induced voltage in the coil
$T_t$	Torque produced by PMSG
$\delta$	Load angle
$E_r$	Air gap emf
$V_t$	Terminal voltage of PMSG
$I_a$	Armature current flowing in PMSG
$R_a$	Machine resistance
$X_L$	Machine leakage reactance
$P_g$	Air gap power
$V_{ph}$	Phase voltage
$I_{ph}$	Phase current
$V_{dc}$	Dc link voltage
$I_{dc}$	Dc link current
$V_{LLmax}$	Line to line peak voltage
$V_o$	Boost output voltage
$V_{in}$	Boost input voltage
$I_L$	Inductor current in boost converter
$I_c$	Current flowing in capacitor connected in boost
$I_o$	Load current in boost converter
$P_{dc}$	Dc link power
$L_c$	Inductance value of inductor in boost converter

# CHAPTER 1

## 1. 1 INTRODUCTION

There are two types of energy sources in the world i.e. renewable energy source and conventional energy sources. Renewable energy sources are the type of energy sources which are plenty in quantity and are derived from earth. Wind energy, solar energy, geo thermal and bio mass are different types of renewable energy sources. These resources are inexhaustible in nature. The known advantages of renewable energy sources are its clean nature, abundant in quantity and most importantly it is ecofriendly unlike non renewable energy sources. Now days more research is going on the enhancement of technology which can efficiently convert the renewable energy sources into useful electrical energy sources. Though the literal conversion efficiency of renewable energy sources is lower than that of conventional energy source, the technology is developed and improvised on daily basis to improve its efficiency above 90%. On the other hand conventional sources of energy are contributing towards pollution, it's depleting in quantity and exhaustible. Because of several disadvantages renewable energy sources can be used as alternatives to it.

Among different types of renewable sources of energy, wind energy is the most cleanest and the efficient source of energy. The major advantages of wind energy are wind-generated electricity doesn't pollute the water, air or soil. It doesn't contribute towards global warming. It doesn't consume large amount of water needed by other energy sources. It is caused by every day solar radiation. Its supply is abundant unlike solar power during bad weather condition and night time. The price of electricity generation by wind power plant is comparatively lesser than other modes of generation. It contributes towards the economy of middle class and low class communities. It also creates employment opportunities for highly skilled workers. It's very fast and easy to install. In a year many large utility scale wind power plants are installed. There are different components of a SWECS, of which the most important is the type of generator used. There are several types of generators used such as Self-excited induction generator (SEIG), doubly fed Induction generator (DFIG) and permanent magnet synchronous generator (PMSG). Among these generators, PMSG has several advantages which make it very usable for WECS. It doesn't require an additional dc supply for excitation circuit. By eliminating the excitation, energy savings of 20% can be had by simply using magnets. It doesn't use slip rings, so it is simpler and maintenance free. The condensers are not required for power factor maintenance unlike in induction generator. It is also advantageous over geared driven segment IG system. Induction generator requires leading reactive power to build up terminal voltage. On other hand DFIG has shorter range of operation unlike PMSG. It is quite

complex management of LVRT in wind farms. LVRT is low voltage ride through capacity of a wind turbine: that is the ability to overcome severe voltage dips on main grid without turning off.

## **1.2 LITERATURE REVIEW**

Non-conventional mode of generation of electricity has several advantages over conventional sources of generation. It is ecofriendly, cost effective, damage free, long lasting and more over harmless [1]. Electricity generation through wind energy is considered as socially beneficial and economically feasible for several applications [2]. For distributed generation system photovoltaic cells, turbines and small scale wind turbines are the main components. In many areas photovoltaic system combined with wind energy system forms a hybrid power system to supply electrical power to the loads as per the requirement [3]. But it is difficult to achieve the optimized efficiency of power conversion as well as maximum reliability of the system [4]. In order to connect to small turbines, permanent magnet synchronous generator, self-excited induction generator, double field excited induction generator are used with gear box.

One of the most efficient wind energy conversion systems is permanent magnet based wind energy conversion system with fixed pitch angle [5]. First the power generated from the SWECS is converter to dc power through diode rectifier which is feed to a boost converter. The boost converter implemented with a MPPT controller optimizes the power of the system. In order to deliver the optimized power to three phase consumer load an inverter can be used at the terminals of boost converter. In case the consumer load increases or wind speed decreases over time, the deficient energy can be delivered by using a battery energy storage system [6]. Other purpose of using a battery energy storage system is to store excess energy [7]. In addition to that to prevent the system from voltage and frequency fluctuation due to overloading, fault occurrence and variable wind speed, voltage frequency controller is brought into the system to maintain constant operating voltage and operating frequency i.e. 50 Hz in this system irrespective of various in operating conditions [8]. The voltage frequency controller also reduces the undesired harmonics in the system. The system also compensates the neutral current flowing in three phase four wire system [12]. Battery energy storage system is connected to the wind energy conversion system to store excess energy or to supply required energy during deficiency in power of the system [13]. The bi-direction converter is implemented to provide a channel for power flow in both direction i.e from system to BESS and vice versa [14]. The active power and reactive power provided by the BESS via voltage source converter stabilizes the terminal voltage as well as system frequency around 50 Hz during adverse situations [15]. The three phase four wire loads, nonlinear loads, dynamic loads are connected to

the WECS. The VF controller is able to maintain system stability with different kind of loads connected to WECS [16].

### **1.3 MOTIVATION**

The total amount of energy produced around the world in one fiscal year is approximately 2.5 lakhs MW. On an average around 10% of energy is stored every year whereas 16% of energy is annual demand of consumers. Hence this deficiency in power has to be compensated by other means of generation. About 60% of energy is produced by using fossil fuels, coals and other raw materials. On the contrary around 12 % of energy is harnessed by means of renewable energy sources such as wind energy, solar energy, geo thermal energy etc. Among these renewable energy sources, about 40 % of energy is produced by wind energy conversion system whereas only 4 % is produced by means of solar energy conversion system. Because of several advantages and high efficiency of wind energy conversion system, the implementation of wind farms is frequent in number. No of researchers have proposed the voltage regulators for PMSG for variable power as well as constant power [1]. However some efforts have been made in the area of controllers for standalone wind energy conversion system using synchronous generators. In WECS, the load on the system varies but reactive power demand of PMSG for maintaining constant voltage is met by battery energy storage system connected to it. In case of wind power generation system, the frequency and system voltage are kept constant. This type of PMSG system requires a load frequency controller as well as voltage controller for maintaining generated power constant. In WECS frequency and voltage vary due to variation in consumer loads as well as due to varying in wind speed, therefore a bidirectional active power and reactive power controller is needed [2]. Various aspects of controller design for synchronous generators are still open for their cost effective utilization and to use renewable energy sources such as wind power for supplying electricity to load and isolated community. Moreover, power quality issues have also become quite relevant due to various types of non-linear and unbalanced loads to be supplied by the PMSG [9].

There has been an extensive work carried out to develop electronic load controllers for isolated synchronous generator for regulating the voltage and frequency [10]. In a typical constant power application, the wind power turbine is uncontrolled and hence it provides a constant power. Thus PMSG has to operate at a constant generated power under varying consumer loads, called single point operation, as the generated power, speed, voltage are constant. Therefore to regulate constant generated power at the generator terminals, electronic load frequency controller or voltage frequency controller is employed using

a voltage source converter and battery energy source system to regulate the system voltage and frequency of the isolated system. The basic principle of PMSG operation is that the total generated power at the generator terminals should be absorbed by the consumer loads and VF controllers to regulate power at the generator terminals to a constant value. Early stage voltage frequency controllers are not having continuous control and the control is implemented in discrete steps. In next stage of development, voltage frequency controllers have been proposed for WECS having continuous control but they are having limitations of feeding various types of loads and problems in power quality as well as distorted generated voltage and currents. Moreover, nowadays to meet the needs of feeding various consumer loads (linear /nonlinear, balanced/unbalanced, 3-phase 4 wires) and maintaining good power quality, extensive improvements have been made on voltage frequency controllers. However, such controllers have disadvantages of complex control and increased cost because of which requirement of an isolated system is lost [11]. However very little literature is available in view of improved power quality, as well as on 3phase-4wire systems therefore the proposed work is aimed on these issues and investigation on some improved electronic load controller.

## **1.4 OBJECTIVE**

Based on the extensive literature review on the topic, following research areas are identified and efforts are made on some of the major issues which are seriously concerned with stand-alone power generation employing permanent magnet synchronous generators (PMSG). The main objectives are

- a) Simulation of PMSG based SWECS
- b) Design and analysis of MPPT controller with Boost converter for PMSG based SWECS
- c) To improve the performance of PMSG based SWECS with closed loop VF control
  - i. During variable wind
  - ii. During load transition
  - iii. During single phase line to ground fault
- d) Simulation of PMSG based SWECS with Battery Energy Storage System (BESS)

### **Simulation of PMSG based SWECS**

Permanent magnet synchronous generator based stand-alone wind energy conversion system is simulated in MATLAB/SIMULINK. The parameters of PMSG & wind turbine are calculated based on the rating of the wind energy conversion system.

## **Design and analysis of MPPT controller with Boost converter for PMSG based SWECS**

Among different types of MPPT control, perturbation and observation (P&O) method of MPPT control is identified as effective controller to extract maximum power during step change in wind speed as this method doesn't need any knowledge of wind speed or need any external sensors for measurement of parameters like voltage and current. The MPPT controller is realized using a boost converter which is connected to a three phase diode bridge rectifier. The dc link voltage and current are taken as input to the controller and the duty cycle is the required output which is then fed to the MPPT controller. A P&O based MPPT controller is modeled and simulated in MATLAB and SIMULINK and tested against PMSG based stand-alone conversion system driven by varying wind speed.

### **To improve the performance of PMSG based SWECS with closed loop VF control**

#### **1. Under variable wind condition**

There are various voltage frequency control scheme such as current synchronous detection (CDS) method and synchronous reference frame theory (SRF) method. The SRF based control scheme is simple in approach and implementation and gives undistorted voltages and currents with less generation of harmonics. The voltage frequency is realized using a three phase voltage source converter (VSC) and battery energy source system (BESS). The method involves the computation of active component and reactive component of reference source current. The controller is modeled and simulated in MATLAB and SIMULINK and tested against PMSG based SWECS driven by varying wind speed. The terminal voltage and frequency are checked for any variation during a step change in wind speed.

#### **2. Under load transition**

Above SRF based voltage frequency is realized in PMSG based SWECS driven by constant wind speed but varying consumer loads. Here for simplicity three phase three wire load is adopted. The load is increased at a specific time and the response of the VF controller as well as SWECS is recorded. The terminal voltage and system frequency are checked for any variation during change in consumer load. BESS provides necessary reactive power during load increment and therefore load power, terminal voltage and frequency remains almost constant.



### **3. Under single phase line to ground fault**

SRF based voltage frequency controller is realized through a three phase voltage source converter (VSC) and battery energy source system (BESS) in PMSG based SWECS driven by constant wind speed. The system response is recorded against sudden occurrence of three phase fault condition at line. The system voltage and frequency are checked for any variation. Battery provides the necessary reactive power through bi-directional voltage source converter during voltage and frequency dip. The system takes few seconds to recover and initial steady state is achieved but with reduced power of the system.

### **Simulation of PMSG based SWECS with Battery Energy Storage System (BESS)**

The wind energy conversion system is connected to a Battery Energy Storage System (BESS) to store as well as supply excess or required energy during variable wind condition, load transition and single phase line to ground fault condition. The system performance is recorded by implementing VF controller using a BESS and VSC.

## **1.5 STRUCTURE OF THESIS**

### **Chapter 1**

The very beginning of the chapter highlights the importance of use of renewable energy source over conventional source of energy. This chapter describes the merits of wind energy as a source of energy and explains about a simple permanent magnet based stand-alone wind energy conversion system. This also includes the motivation and objective of the thesis in a brief manner.

### **Chapter 2**

This chapter deals with the dynamics of a small scale PMSG based wind energy conversion system with MPPT control. It has explained mathematically about different components of a WECS and the need of MPPT control in a SWECS. This chapter has also covered the working principle of MPPT via a boost converter. It also includes the MATLAB simulation of the WECS with MPPT control and the simulation result has been discussed thoroughly with simulation figures.

### **Chapter 3**

This chapter deals with the dynamics of a SWECS with a load voltage and frequency control. It has explained the need of a voltage frequency controller in WECS through several merits and demerits. This chapter has mathematically explained the function of a voltage frequency control using a three phase voltage source converter (VF) and battery energy source system (BESS). It also includes MATLAB simulation of SWECS with VF control for various objectives such as voltage frequency control for variable wind speed, increase in load and fault occurrence at line. This chapter has thoroughly explained the results of simulation using simulation output figures.

### **Chapter 4**

This chapter concludes about SWECS for two types of controller i.e. MPPT controller and VF controller for different operational situations. This includes in detail study about the behavior of the controller response to variation in system parameters. It has covered the need of improvising the existing controlling scheme and future scope of the controller in WECS

## CHAPTER 2

### 2.1 DYNAMICS OF DIFFERENT COMPONENTS OF PMSG BASED SWECS

Wind energy conversion system is consisting of a wind turbine which converts wind energy to mechanical energy. The shaft of the wind turbine is connected to the shaft of the Permanent magnet synchronous generator through a gear box. The gear box provides the rated torque to the generator. The generator develops rated three phase voltages and currents which are then connected to three phase three wire loads.

#### 2.1.1 Wind turbine characteristics

In the wind turbine, the amount of kinetic energy stored can be expressed mathematically as

$$E = \frac{1}{2} \rho A v_w^2 \quad (2.1)$$

Where  $\rho$  = density of air,  $v_w$  is the wind speed in m/s,  $A$  is the volume of air at the cross section of wind turbine. The cross sectional area of the amount of air interacting with the rotor per sec is equal to the cross sectional area of the rotor. The thickness of the air stream is also equal to that of velocity of wind. The power available in the air which is converted into mechanical energy by wind turbine is mathematically given as

$$P = \frac{1}{2} \rho A v_w^3 \quad (2.2)$$

The efficiency of wind energy conversion system is nearly 60 %. It can be analyzed as a part of kinetic energy is delivered to the rotating part and the rest of energy is wasted. The total energy so converted can be mathematically related to power coefficient ( $C_p$ ). The power coefficient  $C_p$  is the ratio of total power converted into mechanical energy to the total power received by the wind turbine. This is shown as mathematically below

$$C_p = \frac{P_{total}}{1/2 \rho A v_w^3} \quad (2.3)$$

Where  $P_{total}$  is the total power received by the wind turbine from wind at intersection. According to Benz's law maximum power that can be harnessed from wind energy is around 59.3% of the total received wind power. It is the maximum value of the power coefficient in wind energy conversion system. Again the power coefficient is a function of many other components such as blade arrangement, rotor blades and setting etc. hence optimized  $C_p$  is obtained by precision and accurate arrangement of these factors. Many different version of power coefficient have been used. The accurate mathematical formula for power coefficient is given as

$$C_p(\lambda, \beta) = 0.5 \left( 116 \frac{1}{\lambda_i} - 0.4\beta - 5 \right) e^{-\left(\frac{21}{\lambda_i}\right)} \quad (2.4)$$

$$\frac{1}{\lambda_i} = \frac{1}{\lambda + 0.08\beta} - \frac{0.035}{1 + \beta^3} \quad (2.5)$$

In this model, the value of the pitch angle of the wind turbine is assumed as zero. The characteristic of power coefficient is a function of tip speed ratio, thrust force and the rotor torque imposed by rotor blades. The thrust force and rotor torque is mathematically described as

$$F = \frac{1}{2} \rho A v_w^2 \quad (2.6)$$

$$T = \frac{1}{2} \rho A v_w^2 R \quad (2.7)$$

Where  $R$  is the rotor blade radius in m. Similarly the ratio between the actual torque developed and theoretical torque is termed as the torque coefficient, which is given as

$$C_T = \frac{T_{Total}}{1/2 \rho A v_w^2 R} \quad (2.8)$$

Where  $T_{Total}$  is the actual torque developed in rotor.

Tip speed ratio is defined as the ratio of velocity of rotor tip and velocity of wind. The power developed by the rotor is a function of tip speed ratio. Mathematically tip speed ratio is given as

$$\lambda = \frac{2\pi NR}{v_w} \quad (2.9)$$

Where N is the rotational speed of the rotor in rpm and R is the radius of the rotor blade in meter and V is the wind speed in m/s. Tip speed ratio can also be expressed as the ratio between power coefficient and torque coefficient.

$$\lambda = \frac{C_p}{C_T} \quad (2.10)$$

The dynamic relation between the rotor and wind stream greatly affects the efficiency of rotor in power extraction. The  $C_p - \lambda$  characteristic shows the rotor performance irrespective of rotor size and site parameters. From Fig 2.5, it is clear that power coefficient increases with increase in tip speed ratio. But when tip speed ratio increases further beyond the optimized value, power coefficient starts to decline at same slope. Hence there is only one optimized point where power extraction is maximum.

### 2.1.2 Two mass drive train

There are two kinds of generators used for small power generation i.e. self-excited induction generator and permanent magnet synchronous generator. The mechanical components such as wind turbine rotates at low rpm whereas the rotor rotates at high rpm. The gear box is used to convert the low speed of wind turbine to the require speed of generator turbine. In multi poles generator system gear box is not necessary. The generator converts the mechanical power to electrical power. The mathematical model for two mass drive train is given as

$$2H \frac{d\omega_t}{dt} = T_m - T_s \quad (2.11)$$

$$2H \frac{d\omega_t}{dt} = T_m - T_s \quad (2.12)$$

$$T_s = K_{ss}\theta_{sta} + D_t \frac{d\theta_{sta}}{dt} \quad (2.13)$$

Where  $H$  is the inertia constant of the triangle,  $\theta_{sta}$  is the shaft twist angle,  $\omega_t$  is the angular speed of the wind turbine,  $\omega_r$  is the rotor speed of the generator,  $\omega_{eb}$  is the electrical base speed,  $T_s$  is the shaft torque, is  $K_{ss}$  the Shaft stiffness,  $D_t$  is the Damping coefficients

### 2.1.3 Permanent magnet synchronous generator (PMSG)

In this kind of generator, the excitation field is supplied by a permanent magnet unlike a coil in synchronous generator. The speed of the rotor and speed of magnetic field is equal to synchronous speed. Hence the name is synchronous. There are two types of rotors i.e. salient pole and cylindrical rotor type. In salient pole rotor type, air gap flux varies with respect to shape of the rotor whereas in cylindrical rotor type, magnitude of air gap flux remains constant. Hence magnetic strength and structural strength is better in case of cylindrical rotors. The windings are embedded in the rotor slots. Cylindrical rotor provides better dynamic balancing than salient pole rotor type. Hence it is used for high speed turbo generators. In salient pole, the rotor poles project outside from the core of rotor whereas cylindrical rotor is used in two or four pole machines. Hence salient pole rotor type is used in low speed hydro electric generators. Salient pole has large no of poles projecting out of core which has large radius but smaller length.

Because of constant air gap flux, the permeance offered to the MMF doesn't depend on the angle between the rotor poles and the MMF axis. In salient pole rotor type, because of variation in air gap flux, the permeance offered to MMF changes with the change in angle between the MMF axis and the rotor poles.

Hence because of several advantages of cylindrical rotor type, it is used very often. Due to constant nature it is simple to model the machine and analyze its functioning. The relationship between EMF frequency and rotor speed is mathematically shown as

$$f = \frac{pn_s}{120} \quad (2.14)$$

Where  $f$  = frequency in Hz,  $n_s$  = speed of the rotor in RPM,  $p$  = no of poles

A synchronous generator when connected to an isolated load behaves as a voltage source whose frequency is measured as a function of its prime mover speed. Synchronous generators are connected in parallel manner through long distance transmission lines. The system is designed to maintain synchronism in spite of electrical and mechanical stress. The merits of such inter-connected system are continuity of supply, capital and are proved to be cost effective. Most of the applications of synchronous motor in industry is

constant speed operation. Another merit of using a synchronous motor is that its power factor can be controlled simply by variation of field current. Hence most of the industries use synchronous motor as loads which are operated at a leading power factor in order to produce high power factor.

### Dynamic model of PMSG

The magnetization curve which is a relationship between  $\phi_f$  and  $F_f$  is linear if the iron is considered to be infinitely permeable. In case of linear magnetization curve the relation can be mathematically shown as

$$\phi_f = pF_f \quad (2.15)$$

Where  $p$  is permeance per pole. The magnitude of the EMF induced in the coils of  $N$  no of turns is given by faraday's law

$$e_{af} = -N \frac{d\lambda}{dt} \quad (2.16)$$

$$e_{af} = N\omega_s \phi_f \sin \omega_s t \quad (2.17)$$

$\lambda$  is flux linkage of one coil. The RMS value of induced EMF in the coil is given as

$$E_f = \sqrt{2}\pi f N \phi_f \quad (2.18)$$

Where  $\phi_f$  is flux per poles. The magnitude of torque is given as

$$T_t = \frac{\pi}{2} \left(\frac{p}{2}\right)^2 \phi_r F_f \sin \delta \quad (2.19)$$

Where  $\delta$  is the angle by which  $F_f$  leads  $F_r$ .

During motoring action the positive current flows in opposite direction to the direction in which the induced emf is yielded. The electromagnetic torque acts on the field poles in the direction of rotation so that the mechanical power is produced hence it is operating as a motor. On other hand, if the terminal voltage is same as air gap emf i.e.  $V_t = E_r$  and its frequency is held fixed by an external 3 phase source called infinite bus, the machine acts as a generator or motor depending upon the mechanical condition at the shaft. The circuit diagram of the machine acting as a generator is drawn below. The dynamic equation related to the generating mode of operation is mathematically given as

$$V_t = E_r - I_a(R_a + jX_L) \quad (2.20)$$

Where  $R_a$  is the machine resistance,  $X_L$  is leakage reactance in series with the resistance between the terminal voltage and air gap EMF for each machine phase

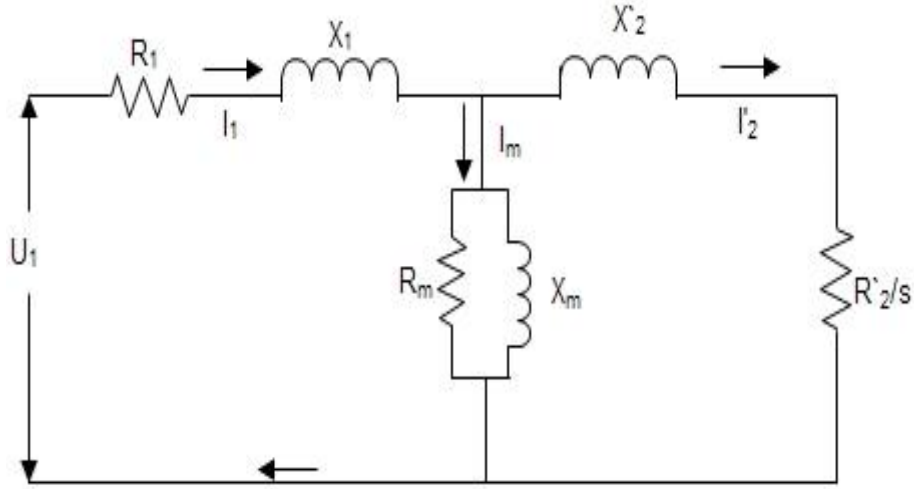


Fig 2.1 Circuit diagram of Permanent Magnet Synchronous Generator

#### 2.1.4 AC to DC three phase diode rectifier

When generated power is converted to dc power at unity power factor, the mathematical dynamic equation is given by

$$P_g = 3V_{ph}I_{ph} = V_{dc}I_{dc} \quad (2.21)$$

Where  $P_g$  is the generated power,  $V_{ph}I_{ph}$  are the phase voltage and current and  $V_{dc}I_{dc}$  are the rectified dc voltage and current.

The value of average power is equal to

$$V_{dc} = \frac{3}{\pi} \int_{-\pi/6}^{\pi/6} V_{LLmax} \cos \theta d\theta = \frac{3}{\pi} V_{LL} \quad (2.22)$$

Where  $V_{LLmax}$  is peak value of line to line input voltage of rectifier. Furthermore, the relation of rectified voltage and RMS phase voltage is:



$$V_{dc} = \frac{3}{\pi} \sqrt{6} V \quad (2.23)$$

### 2.1.5 Boost Converter

The three phase voltages are converted to the DC voltage via a three phase rectifier circuit using a universal Simulink block. The rectified dc voltage is then supplied across the DC-DC Boost converter. The duty cycle of the boost converter is controlled by a MPPT controller. Hence optimized boosted DC voltage is produced at the output port of Boost converter A boost converter is used as the power interface between the WECS and the load to achieve maximum power. The output voltage dc  $V_o$  of the boost converter can be expressed as:

$$V_o = \frac{V_{in}}{1 - d} \quad (2.24)$$

Where  $d$  is the duty cycle,  $V_o$  is the output dc voltage from boost converter and  $V_{in}$  is the input dc voltage to the boost converter. It can be seen the input DC voltages  $V_{in}$  can be shifted to a high level. This power converter is suitable for a lower WECS output voltage and higher desirable DC link voltage case.

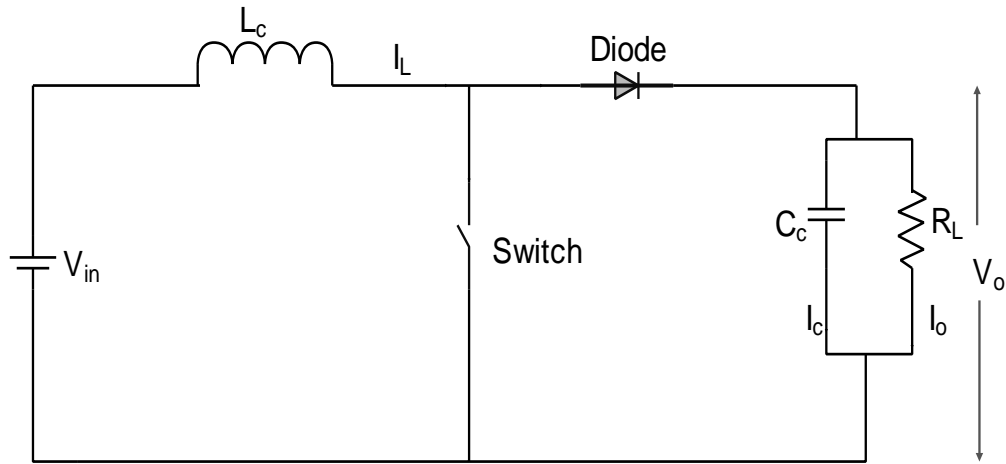


Fig 2.2 Circuit diagram of a boost converter

### 2.1.6 MPPT Controller

Maximum power point tracking is an efficient method of extracting generated power from the generating systems used by grid connected inverters, solar battery chargers, wind energy conversion system. The MPPT controller implements the P&O control technique in order to provide the required duty cycle to the boost converter. Which produces optimized DC link voltage and hence maximum power is generated by the generator. Wind energy is dependent on weather, topology and environment. It is essential to choose the best place where quality of air can produce more electricity. Then it is difficult to wind turbine to provide 60% of power wind speed. Wind energy conversion system have also other losses like mechanical friction and low generator's efficiency. So the amount of power output from WECS depends to the tracked wind power. Therefore, a maximum power point tracking control is required.

#### Types of MPPT techniques

##### a) Optimal torque control (OT)

As discussed in TSR MPPT method of control, maintaining the operation of the system at optimized TSR ensures maximum conversion of the available wind energy into mechanical energy. It can be seen from Fig 2.3, that the objective of this method is to adjust the PMSG torque in reference to maximum power reference torque of the wind turbine at a given wind speed. The turbine power as a function of  $\lambda$  and  $\omega_r$  is determined mathematically. The block diagram as shown in Fig 2.3 describes the working of the OT controller.

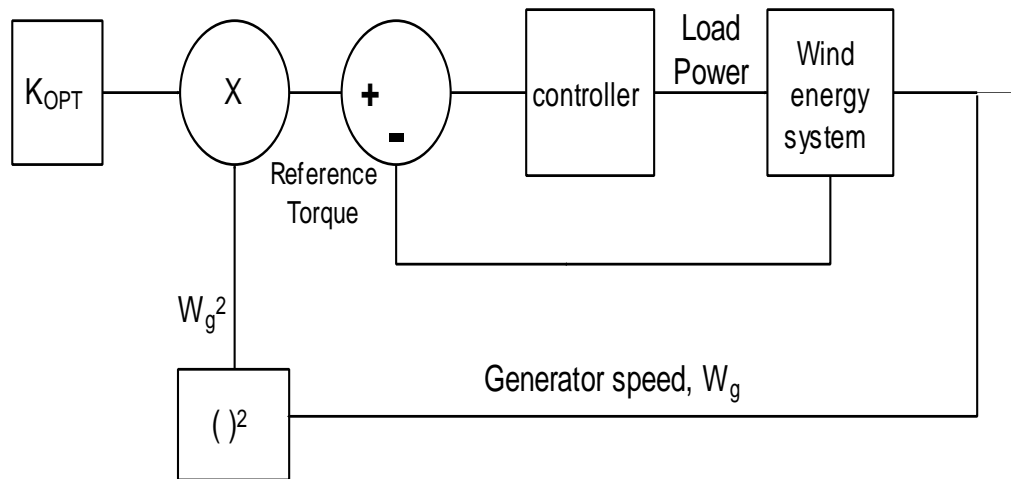


Fig 2.3 Block diagram for optimal torque control [2]

### b) Power signal feedback control (PSF)

In this controlling method the reference optimum power curve of the wind turbine is obtained first from the experimental results. The operating points for maximum output power and the corresponding wind turbine speed are saved in a lookup table. The block diagram of power signal feedback control is shown in Fig 2.4.

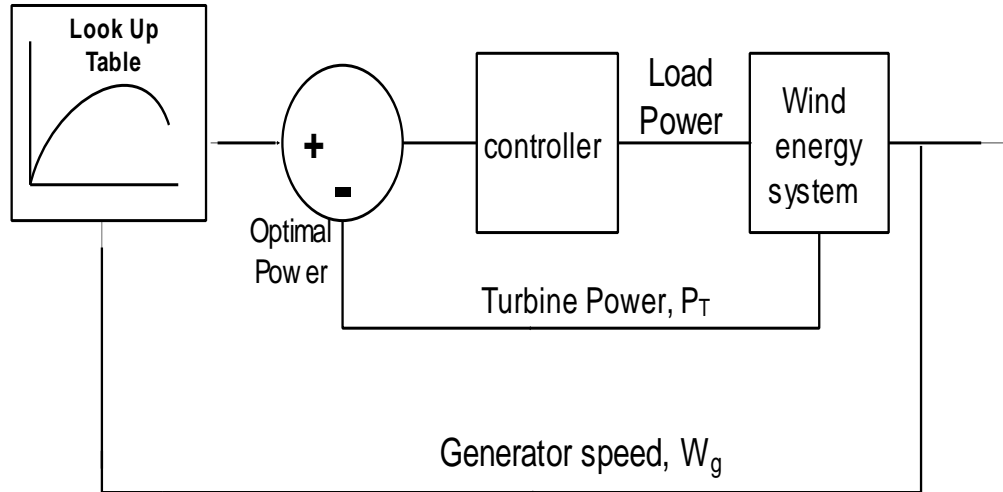
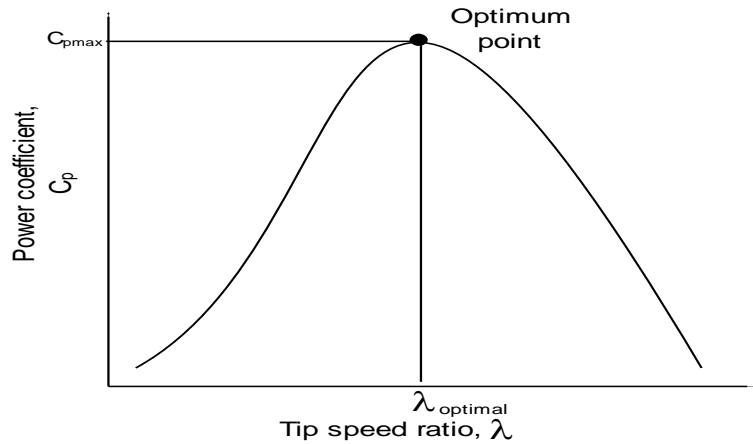


Fig 2.4 Block diagram for PSF MPPT control [2]

### c) Tip speed ratio (TSR) control

The optimal TSR is constant for a given wind turbine irrespective of variable wind speed as shown in Fig 2.5. When the wind turbine operates at this optimal TSR, the power so extracted from the WECS is maximized. Hence MPPT method forces the energy conversion system to operate at optimized TSR by comparing it with the actual value and supplying this error to the MPPT controller. The system responds by changing the generator speed to reduce this error. This optimized TSR can be computed experimentally and used as a reference. Though this method is simple as wind speed is measured directly, a precise measurement for wind speed is not possible and also the cost of the system increases. The block diagram of the tip speed ratio control method is shown in Fig 2.6.



**Fig 2.5 plot of power coefficient Vs tip speed ratio [1]**

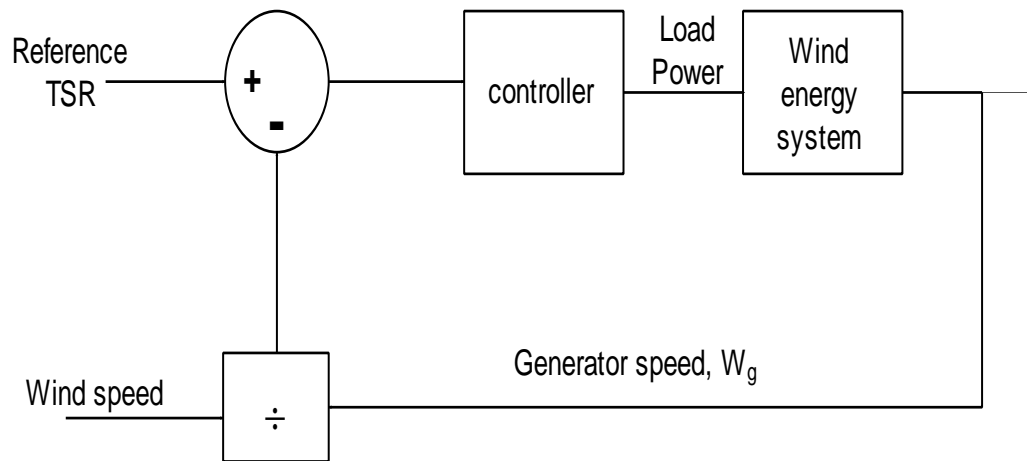


**Fig 2.6 Block diagram for Tip speed ratio MPPT control [2]**

#### **d) Perturbation and observation control (P&O)**

The perturbation and observation method of control is an efficient optimization method which uses the principle of searching for the local optimum point of a given function. It is used to search the optimal operating point and hence it will help to maximize the extracted energy. This control technique is based on introducing a small step size variation in a control variable and observing the changes in the target function till the slope of the function becomes zero. As shown in Fig 2.7, the controller guides the operating point by locating the position and the distance of the operating point from the peak point. The operating point moves towards right if it is in extreme left side and vice versa. In this method the duty cycle of the boost converter is perturbed and the dc link power is observed. In this method wind speed

measurement is not required hence the mechanical sensors are not used. Therefore this method of control is more reliable and cost effective.

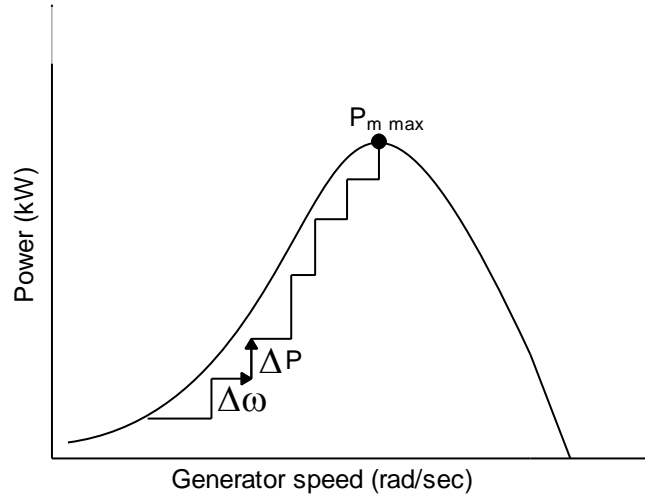


Fig 2.7 Plot of generated power in kW Vs. Generator speed in rad/sec [1]

### Concept analysis of MPPT control technique

The MPPT process in proposed system is based on directly adjusting the dc/dc boost converter duty cycle. In a fixed step size based P&O method, in order to reduce oscillation around the peak operating, we can change the value of duty cycle of the converter by introducing the step size i.e.  $\Delta D$  at each sample based on the working condition. The maximum power point of operation is obtained mathematically when the condition is satisfied i.e.

$$\frac{dP_{dc}}{dV_{dc}} = 0 \quad (2.25)$$

Where  $P_{dc}$  is the dc link power and  $V_{dc}$  is the dc link voltage. Like the power vs. speed graph, the function  $P_{dc}(V_{dc})$  has also a single operating point where maximum power can be achieved. This indicates that tracking of maximum power can be performed by step by step searching the rectified dc power rather than measuring the environmental conditions such as wind speed. A simple wind energy conversion system with MPPT control is shown in Fig 2.14 which is simulated in MATLAB and SIMULINK to test the efficiency and effectiveness of the proposed MPPT control method.

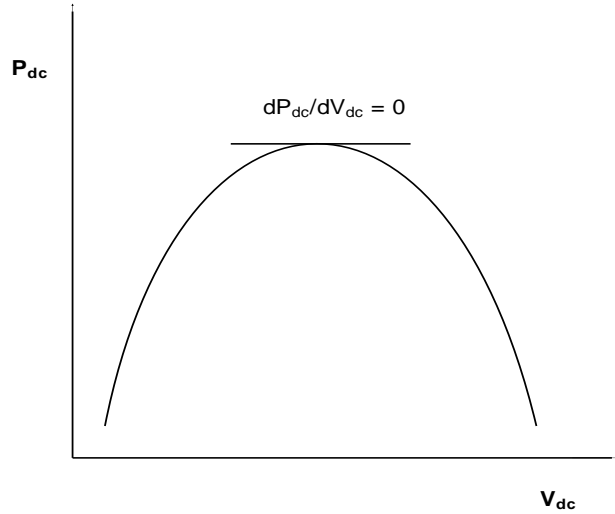


**Fig 2.8 Plot of dc link power vs dc link voltage [3]**

From above Fig 2.8, it is clear that as the duty-cycle adjustment is guided by the direction of slope of the function i.e.  $\frac{dP_{dc}}{dV_{dc}}$ , the duty-cycle value is increased in the high-speed side of the WG characteristic. Hence WG rotor-speed decreases and power increases till the controller reaches the Maximum Power Point is reached. In the same way when the starting point is in the low-speed side, following the direction of slope of the function i.e.  $\frac{dP_{dc}}{dV_{dc}}$  which results in decrease of the value of duty cycle. Hence the WG rotor speed is gradually and the controlling variable subsequently converges at the MPP.

#### **Flow chart for MPPT algorithm**

Flow chart describes the step by step working of a MPPT controller based on the describe algorithm. As shown in Fig 2.9, the inputs taken are the dc link voltage and current and output is the required duty cycle. In the second step, the controller is computing the dc link power by multiplying mathematically the input dc link voltage and current. The next step explains (n-1)th value of dc link power which is obtained by using a delay function in Simulink. If the difference in nth and (n-1)th value of dc link power is greater than zero then the algorithm goes forward and computes the difference in dc link voltage. Accordingly the difference in dc link voltage generates new duty cycle by adjusting delta D which is added or subtracted as per the conditions applied.

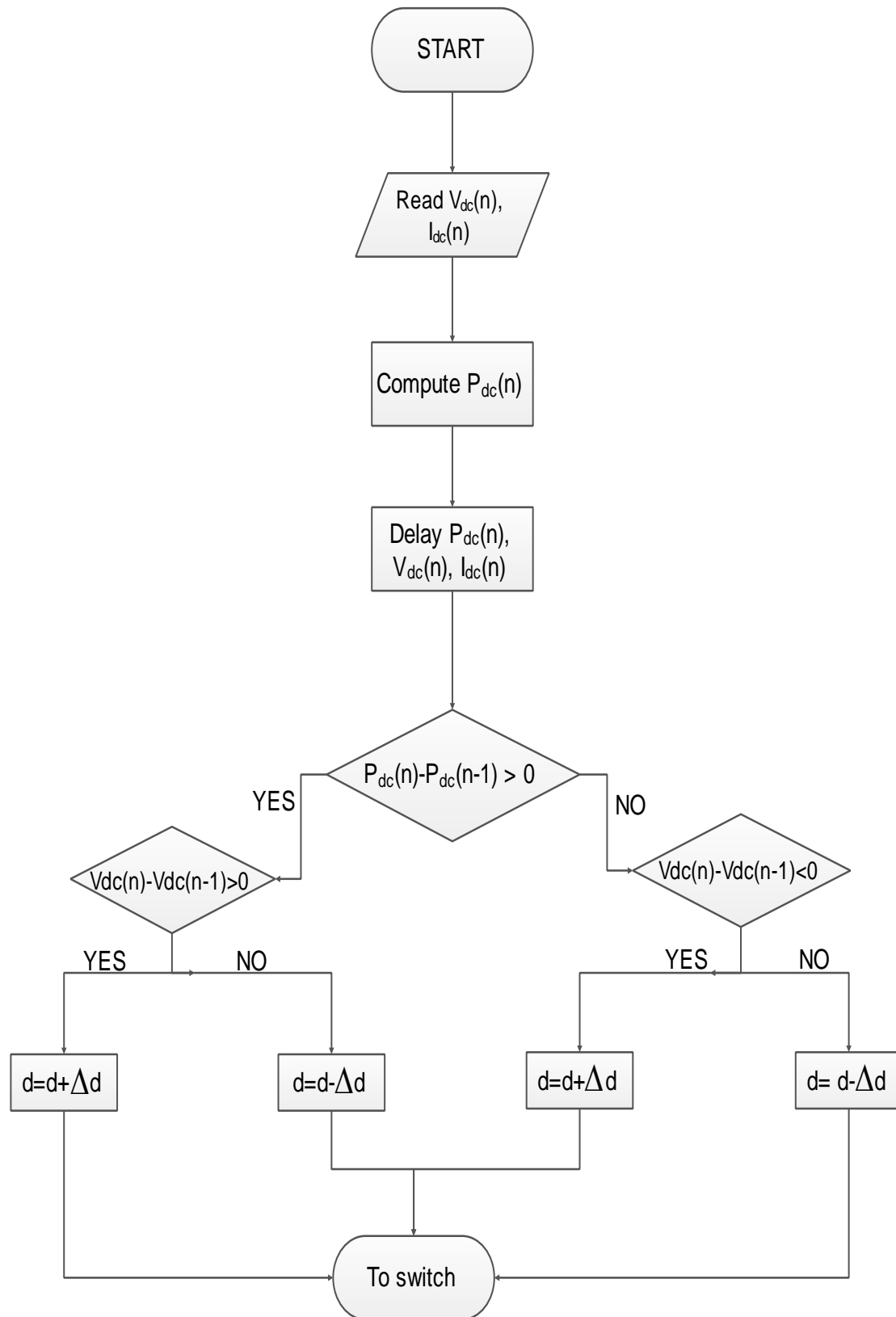


**Fig 2.9 Flow chart for P&O MPPT control**

### Implementation of MPPT using a boost converter

Boost converter is used often for practical purpose in order to step up low dc voltage to high dc voltage. The output voltage is a function of duty cycle which is the ratio of ON time period and total time period of the pulse used to trigger the operating switch. The block diagram shown in Fig 2.10 gives an overview of the required implementation.

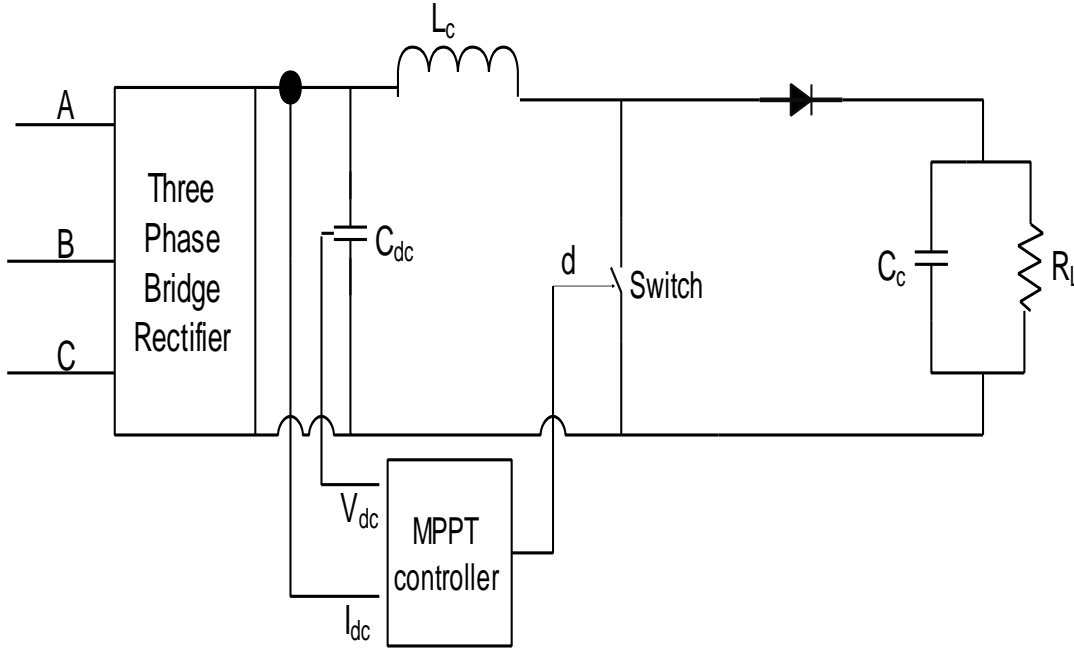


Fig 2.10 Circuit diagram for boost converter with MPPT controller

## 2.2 SIMULATION OF PMSG BASED SWECS WITH MPPT CONTROL

### 2.2.1 Two mass drive train

The purpose of using gearbox in the wind energy conversion system is that different mechanical parts need to run at different speeds for efficiency. Some parts of the generating system run fairly faster than other mechanical parts since the generated voltage is a function of rate of change of magnetic fields. In contrast to that the turbine blades rotate slower than other mechanical parts since they will fail to take centrifugal stress. Hence gear box is essential to speed up the slow turbine rotations to the faster generator rotations. Fig 2.11 shows the Simulink model of two mass drive train.



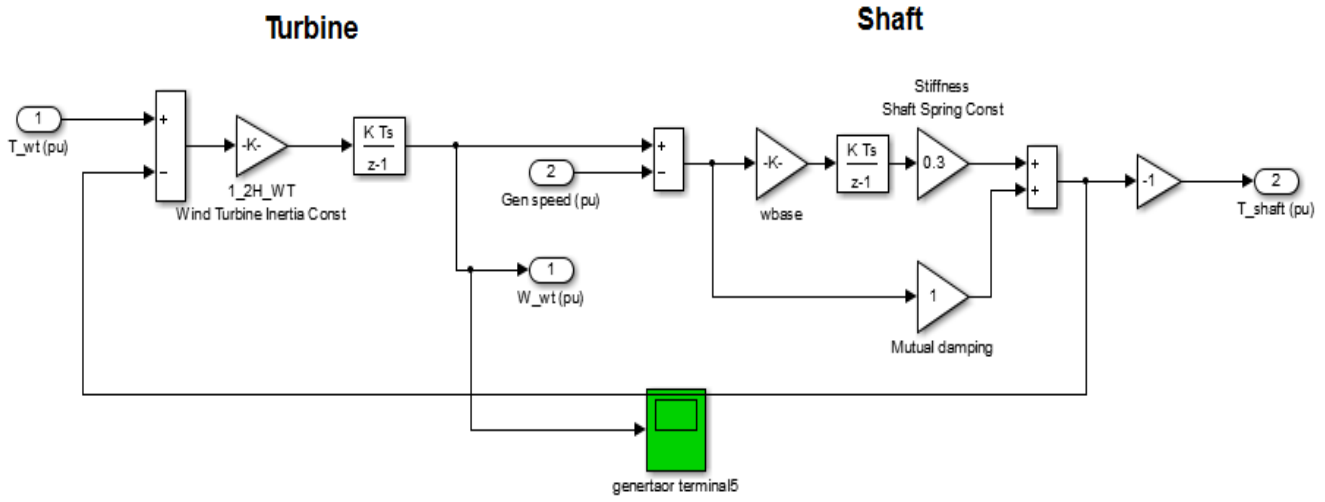


Fig 2.11 Simulink model diagram for two mass drive train

## 2.2.2 Wind turbine, two mass drive train and PMSG

To produce rated three phase ac voltages and currents, the generator should be provided with rated input torque. This rated input torque is provided by the wind turbine through a two mass drive train which serve as a gear box between generator and turbine as shown in Fig 2.12. The per unit rotor speed is supplied as input to the two mass drive train. The values of different parameters of PMSG & wind turbine are shown in Table 2.1 and Table 2.2 respectively.

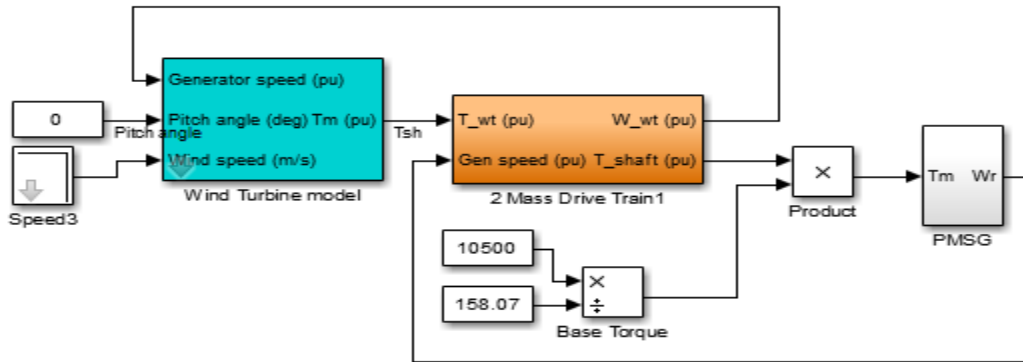


Fig 2.12 Simulink model for wind turbine, two mass drive train and PMSG

**Table 2.1 PMSG parameters**

Variables	Specifications
Rating	10.5 kW
Stator resistance	0.434 ohm
Armature inductance	0.000834H
Flux linkage	0.5
Inertia	0.001197J
Damping	0.001189F
Poles pair	2

**Table 2.2 Wind turbine parameters**

Variables	Specifications
Nominal mechanical power	10.5KW
Base power of generator	10.5/0.9 KVA
Base wind speed	0.8
Base rotational speed	1.2
Pitch angle	0

### 2.2.3 Boost converter

The three phase ac voltages from the PMSG are rectified using a three phase diode rectifier. This rectified dc voltage serves as an input to the boost converter. The values of different components of boost converter are shown in Table 2.3. The gating pulse to the IGBT switch is provided by a PWM generator which is a function of duty cycle (Fig 2.13).

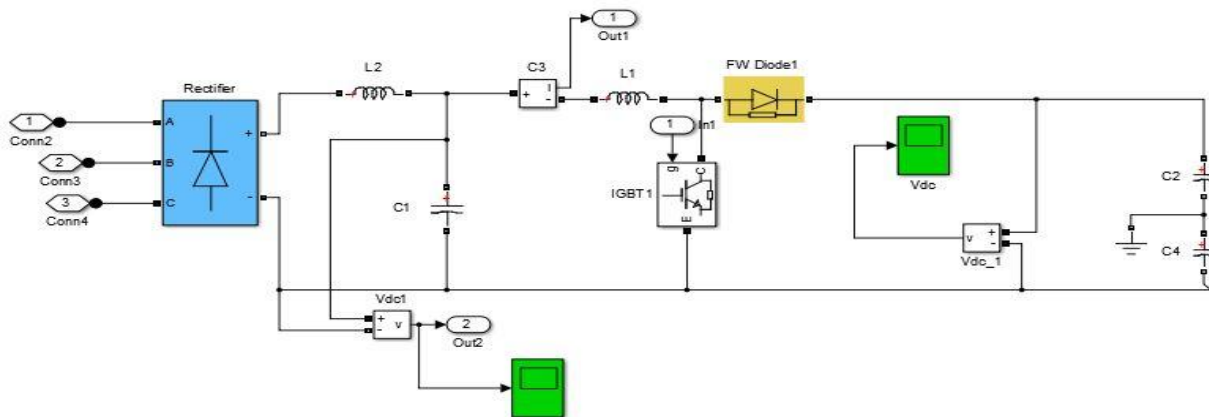


**Fig 2.13 Simulink diagram for Boost converter**

The boost converter parameters are inductor and capacitor. The value of inductor and capacitor for switching frequency of 25 kHz, duty cycle of 0.67 and load resistance of 30 ohm is obtained as

$$L_c = \frac{(1 - k)kR}{2f_s} = 133\mu H \quad (2.26)$$

$$C_c = \frac{k}{2fR} = 0.44\mu F \quad (2.27)$$

**Table 2.3 Boost converter parameters**

Variables	Specifications
C <sub>c</sub>	0.44μF
C <sub>2</sub>	0.8μF
C <sub>4</sub>	0.8μF
L <sub>c</sub>	133μH
L <sub>2</sub>	0.7mH

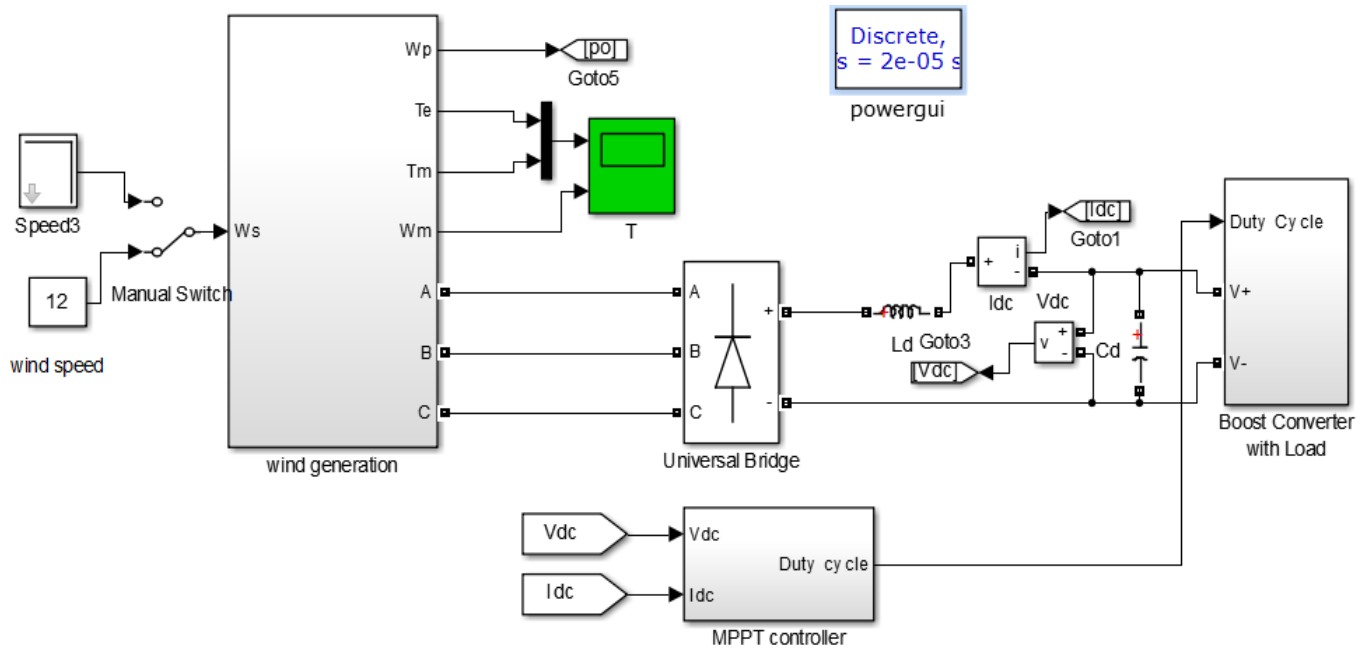


**Fig 2.14 Simulink model of SWECS with MPPT control**

## 2.3 SIMULATION RESULTS

The simulation of PMSG based SWECS with MPPT control is carried out with step change in wind speed. The initial value of wind speed was 8 m/s. Due to step change at  $t = 2$  secs, the wind speed increased to 12 m/s which is high enough to produce more power from PMSG. As a result the generated voltages, source current, wind power, DC link voltage and current increases. The following figures describe the responses of different parameters to step change in wind speed.

In this MPPT control though the output power has increased but it's not the optimized power. Fig 2.15 shows the step change in wind speed from 8 m/sec to 12 m/sec at  $t = 2$  secs.

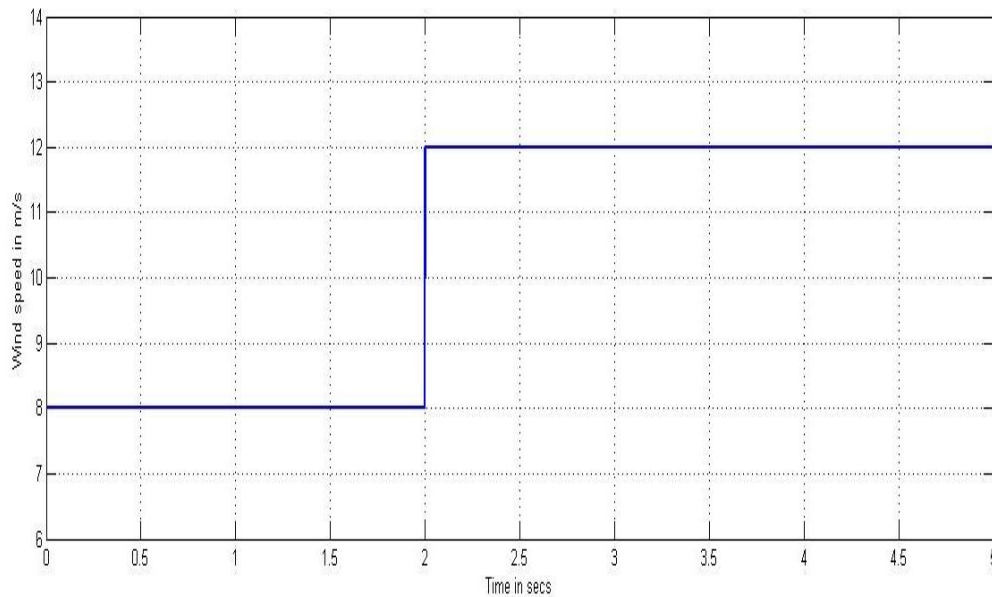


**Fig 2. 15 Variable wind speed**

When the wind speed is 8 m/sec, output generated power without MPPT control is around 1.5 kW. After wind speed increases to 12 m/sec, the output generated power without MPPT control is around 4.2 kW. Now with MPPT control, the generated power during low wind speed is around 2.2 kW and during high wind speed is around 6 kW. Fig 2.16 clearly shows the difference in generated output power with and without MPPT control. The red plot indicates the output power with MPPT control whereas the blue plot indicates the generated power without MPPT control.

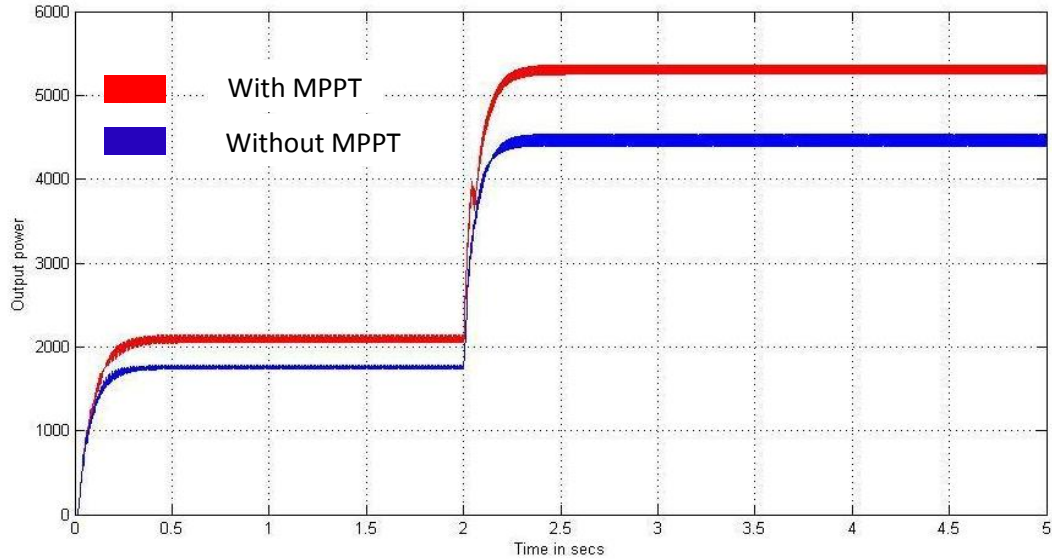


**Fig 2. 16 Output generated power of PMSG**

Before change in wind speed i.e. at wind speed of 8 m/sec, the dc link voltage without MPPT control is around 220 V whereas after increase in wind speed to 12 m/sec at  $t = 2$  secs, the DC link voltage without MPPT control is around 350 V. Similarly before change in wind speed, the DC link voltage with MPPT control is around 260 V and after increment in wind speed to 12 m/sec, the DC link voltage with MPPT control is around 420 V. The figure below (Fig 2.17) shows the DC link voltage before and after change in wind speed.

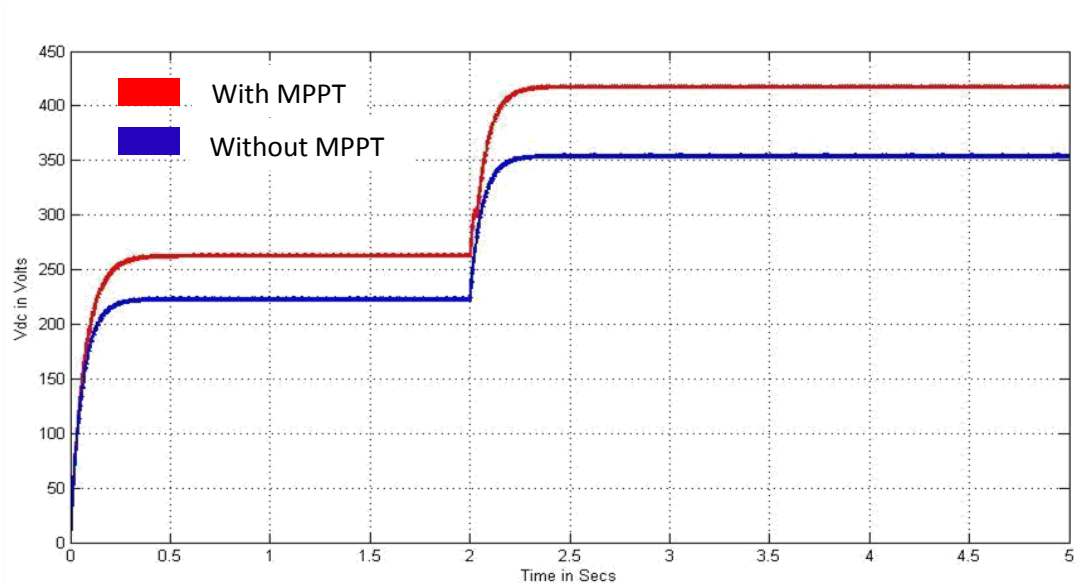


**Fig 2. 17 Dc link voltage of boost converter**

Before change in wind speed, the rotor speed without MPPT control is around 60 rad/sec. At  $t = 2$  secs, the wind speed increases from 8 m/sec to 12 m/sec. Hence the rotor speed without MPPT control after step change in wind speed is around 100 rad/sec. Similarly with MPPT control the rotor speed before change in wind speed is around 75 rad/sec and after change in wind speed is around 118 rad/sec. The following diagram (Fig 2.18) shows rotor speed in rad/sec unit.

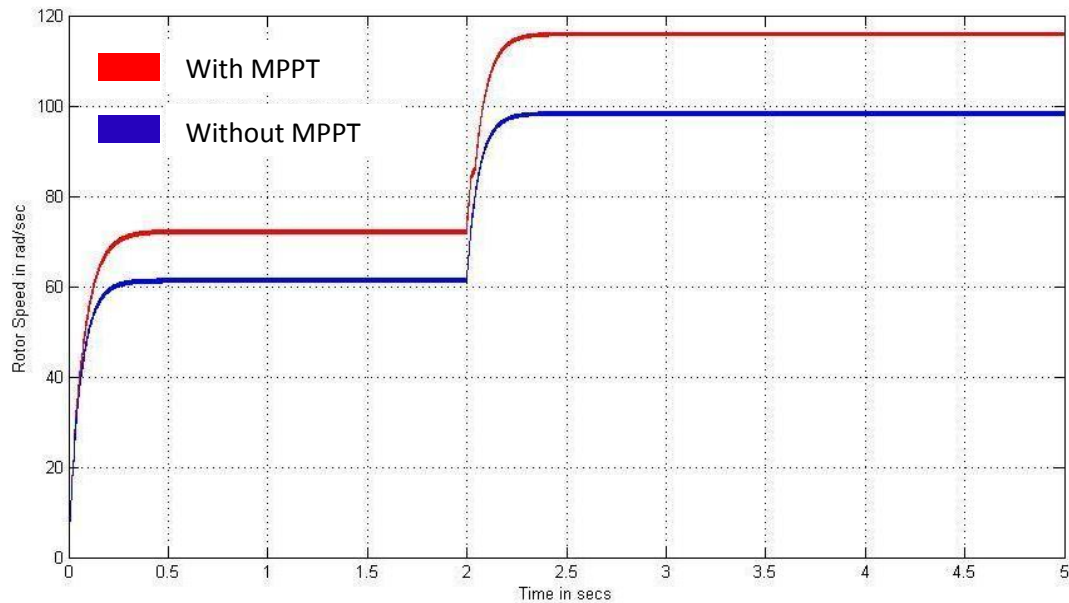


**Fig 2. 18 Rotor speed of PMSG**

## CHAPTER 3

### 3.1 OVERVIEW ON VOLTAGE FREQUENCY CONTROLLER

The Voltage Frequency controller is realized using a bi-directional voltage source converter connected to battery storage system. Battery Energy Storage System (BESS) is a self-charging as well as discharging circuit used to store excess energy or supply energy to compensate deficiency in energy of the system. Fig 3.1 describes the overall SWECS with VF control. There are two components to be computed i.e. active component of the reference source current and the reactive component of the reference source current. The PI controllers are used to make the steady state errors zero and stabilize the signals. The output terminals of the VF controller provide three phase reference source currents. There are several factors that adversely cause voltage as well as frequency fluctuations. Location of the distribution line, over loading to a small distribution grid, voltage imbalances, load factor on transmission and distribution system are few major problems that trigger voltage and frequency fluctuation. There are also several disadvantages of frequency fluctuation such as speed of three phase ac motor which directly depends upon system frequency varies which degrades the motor performance, excessive vibration, noise and mechanical stress on the system as well as turbine blades, damage of retrieval process and digital storage. Hence using a voltage and frequency controller will force the equipment to operate within voltage levels, provision of phase to phase voltage balancing, reduction in unwanted heat generated in motors.

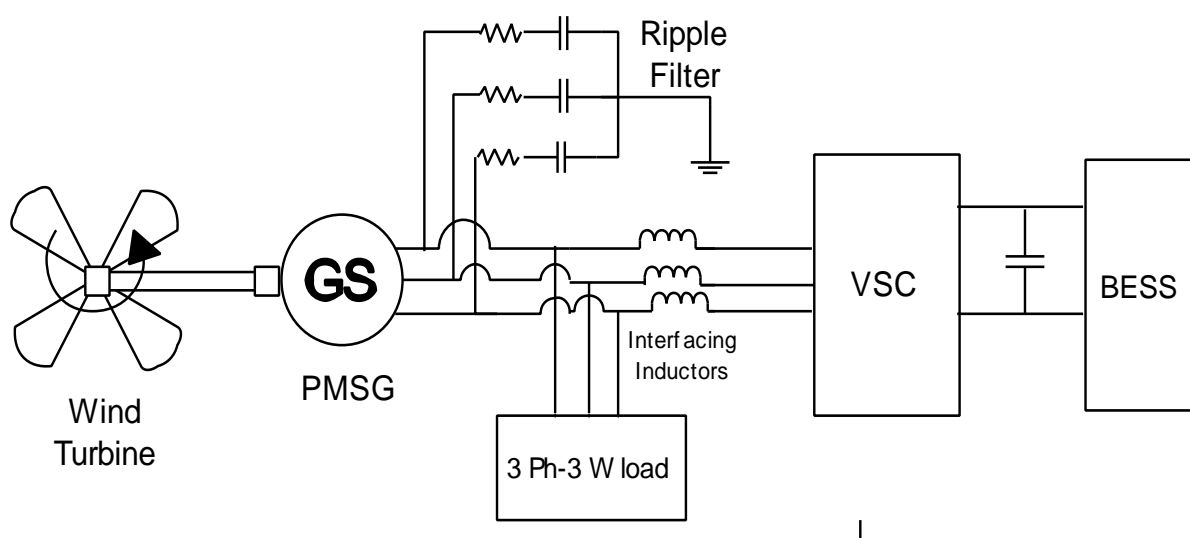


Fig 3.1 Circuit diagram for VF controller using VSC and BESS connected to PMSG [2]

### 3.1.1 Types of voltage frequency control schemes

#### a) Current synchronous detection based control algorithm (CSD):

The control method is used for the VFC of SWECS feeding three phase three wire loads. The principle of this method is to compute the reference source current by using the controlling scheme and use it to determine the error. Reference source currents are computed by calculating the active and reactive components of the reference source currents. The in-phase and phase shifted templates are determined by estimating the PCC voltage amplitude and instantaneous phase voltages amplitude by the formula given as below

$$V_t(n) = \sqrt{2/3(v_a^2 + v_b^2 + v_c^2)} \quad (3.1)$$

Three phase locked loop is used to determine SWECS frequency. It requires a sample and hold logic, an instant crossing detector and an estimated phase shifted voltage. For estimation of reference source active power, the load active power drawn is subtracted from the output of the frequency PI controller i.e.

$$P_g^* = P_f(n) - P_L(n) \quad (3.2)$$

The output of voltage PI controller is subtracted from load reactive power to determine the reactive component as

$$Q_g^* = Q_{vq}(n) - Q_L(n) \quad (3.3)$$

The reference source currents are compared with sensed source currents of each phase. The resulting current errors are amplified and compared with constant high frequency triangular carrier waves which generate switching signals for the switches of VFC of SWECS.

#### b) Synchronous reference frame theory based control algorithm (SRF):

This control technique is different from that of CSD technique. Unlike CSD method, here terminal voltage amplitude and system frequency is used as reference values. This method works on the principle of synchronous frame theory in which three phase load currents are first converted to two phase d-q axis using a PLL. Low pass filters are used to completely eliminate harmonics and unwanted ac components in d-q components. The filtered d and q components are differentiated from respective outputs of PI



controller. The d axis component of load current along with output of frequency PI controller constitutes the reference d axis component of source current. Whereas q axis of load current along with output of voltage PI controller constitutes the q axis reference component of source current. The respective d-q axis components of reference source currents are converted to three phase reference source current by using reverse park's theorem.

### 3.1.2 Implementation of a Voltage Frequency controller using a VSC and BESS

A three-leg VSC with a BESS at its DC bus is used as a VF Controller. The mid-point of each leg of a VFC is connected at the point of common coupling (PCC) through an interfacing inductor. The VSC-based VFC regulates the SWECS frequency under change in wind power or consumer loads by supplying the deficit load active power. A configuration of a PMSG-based SWECS to feed 3P3 W load, is shown in Fig. 3.1. The presence of permanent magnets at rotor terminals allows rated field excitation. Under change in wind speed, the required reactive power is made available to the PMSG through a VSC of VFC. The VSC-based VFC also provides deficit load reactive power and an active power in the presence of a BESS to keep constant system frequency. A high-pass RC ripple filter is used at the PCC to absorb switching ripple.

## 3.2 DYNAMICS OF VOLTAGE FREQUENCY (VF) CONTROLLER, VSC AND BESS

### 3.2.1 Voltage Frequency Controller (VFC)

Voltage frequency controller is realized using a battery energy storage system and a bi-direction voltage source converter. The controller implements an algorithm which is based on synchronous reference frame theory (SRF). The main objective is to compute reference source currents. The load currents and the terminal three phase generated voltages are sensed as feedback signals and used for mathematical computation of amplitude of terminal voltage and system frequency. The load currents are transformed from a-b-c to the d-q frame using park's transformation.

$$\begin{bmatrix} Vd \\ Vq \end{bmatrix} = \frac{2}{3} \begin{bmatrix} 1 & -\frac{1}{2} & -\frac{1}{2} \\ 0 & \frac{\sqrt{3}}{2} & -\frac{\sqrt{3}}{2} \end{bmatrix} \begin{bmatrix} Va \\ Vb \\ Vc \end{bmatrix}$$

The three phase voltages from load is converted into two phase dc components i.e. d axis and q axis component using the unit vectors so obtained. In order to filter the undesired ac harmonic components, low pass filters are used. The fundamental components along with harmonic components are given as:

$$i_{ld} = i_{ddc} + i_{dac} \quad (3.4)$$

$$i_{lq} = i_{qdc} + i_{qac} \quad (3.5)$$

The fundamental components so obtained after passing through low pass filters are  $i_{ddc}$ ,  $i_{qdc}$ .

#### **Estimation of active component of reference source current:**

Using three phase load currents as input to PLL, fundamental frequency of the system is obtained. The computed frequency of the SWECS is compared with the reference frequency i.e. 50 Hz and the error is passed through a PI controller. The output of the pi controller is assumed as the active current to be drawn by the battery energy storage system and voltage source converter. The dynamics of the PI controller is given as:

$$i_{db(n)} = i_{db(n-1)} + k_{pd}(f_{e(n)} - f_{e(n-1)}) + k_{id}f_{e(n)} \quad (3.6)$$

Where the frequency is given as  $f_e(n) = f - f(n)$ . the PI controller's parameters i.e.  $K_{pd}$  and  $K_{id}$  are estimated by hit and trail method. The total reference d-axis source current is therefore as,

$$i_{sd}^* = i_{ddc} - i_{db} \quad (3.7)$$

#### **Estimation of the reactive component of the reference source current:**

The main objective is to estimate the reactive component of reference source current. The input to the PI controller is the voltage error whereas the output of the voltage PI controller produces current which is equivalent to the quadrature axis component of the source current. The resultant of addition of quadrature axis component and the component obtained from the voltage PI controller ( $i_{qr}$ ) is assumed as the quadrature axis component of source current. The amplitude of the terminal voltage is calculated as

$$V_t(n) = \sqrt{2/3(v_a^2 + v_b^2 + v_c^2)} \quad (3.8)$$

Then, a PI controller is used to minimize this voltage error and drive terminal voltage towards the reference value i.e. 320 V. The dynamics of the voltage PI controller is described as

$$i_{qr(n)} = i_{qr(n-1)} + k_{pq}(v_{se(n)} - v_{se(n-1)}) + k_{iq}v_{en} \quad (3.9)$$

Where,  $v_{s(n)} = v_s^* - v_{s(n)}$  indicates the error between reference voltage ( $v_s^*$ ) and sensed ( $v_{s(n)}$ ) terminal voltage at the nth sampling instant.  $K_{pq}$  and  $K_{iq}$  are the proportional and the integral gains of the voltage PI controller. The reference source quadrature axis current is given as

$$i_{sq}^* = i_{qdc} + i_{qr} \quad (3.10)$$

### Computation of reference source currents

The obtained d-q components of reference source currents are converted from d-q-0 frame to the a-b-c frame using the reverse Park's transformation where the unit vectors are obtained from three phase load currents by using a three phase locked loop(PLL). Fig 3.2 highlights the principle of SRF based VF control.

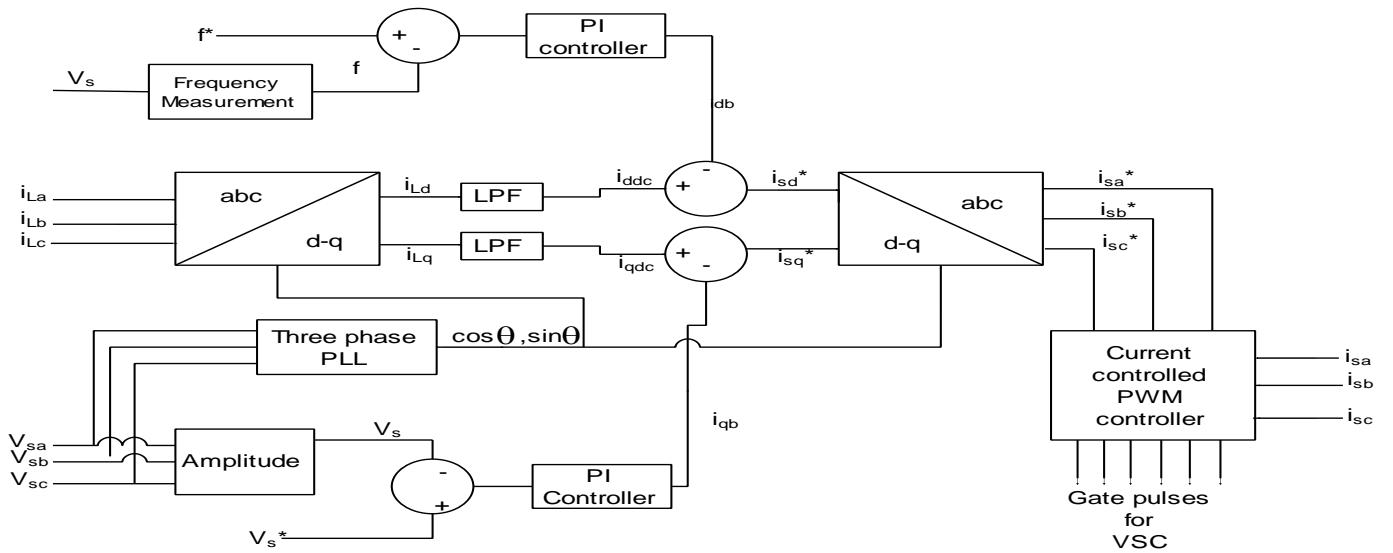


Fig 3.2 Block diagram of SRF technique of VF control [2]

### 3.2.2 PWM generator

In a PWM current controller, the sensed three phase source currents and the reference source currents so obtained by above method are compared and the error in each phase is processed through PWM generator. These current signals are compared with a triangular carrier signal of high frequency about 5 kHz in a PWM and the gating signals are generated for six IGBT switches of VSC of the VF controller as shown in Fig 3.3.

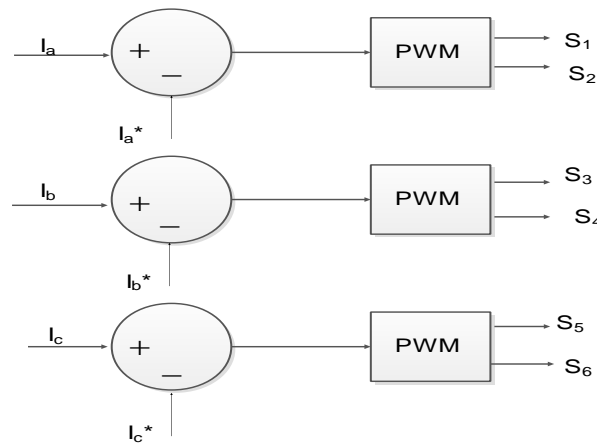


Fig 3.3 PWM generator

### 3.2.3 Voltage Source Converter (VSC)

The three phase ac voltages from PMSG are connected to the six leg three phase voltage source converter via interfacing inductors. The VSC is built of six IGBT switches with diode in anti-parallel manner as shown in Fig 3.4. The gating pulses are provided by three single phase current controlled PWM generators. The reference to these PWM generators is the difference between the reference source current and computed source current.

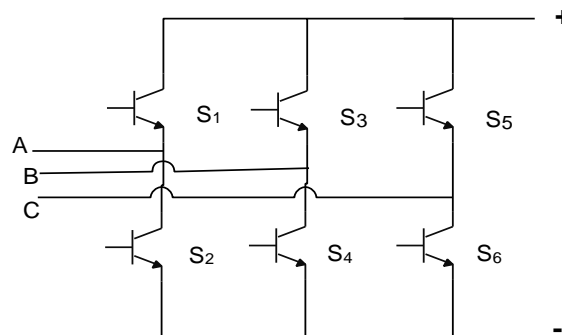


Fig 3.4 Circuit diagram of VSC

### 3.2.4 Battery Energy Storage System (BESS)

Battery energy storage system consists of a rechargeable battery with circuit parameters as resistor and capacitors as shown in Fig 3.5.  $R_{in}$  is the equivalent series resistance of the series combination of battery, which is usually a small value (considered 0.001 ohm). The parallel circuit of  $R_b$  and  $C_b$  is used to describe the stored energy responsible for self-discharging. The battery parameters to be computed are battery nominal voltage and parallel circuit capacitance and resistance.

## 3.3 SIMULATION OF VF CONTROLLER, VSC AND BESS

### 3.3.1 Battery energy storage system (BESS)

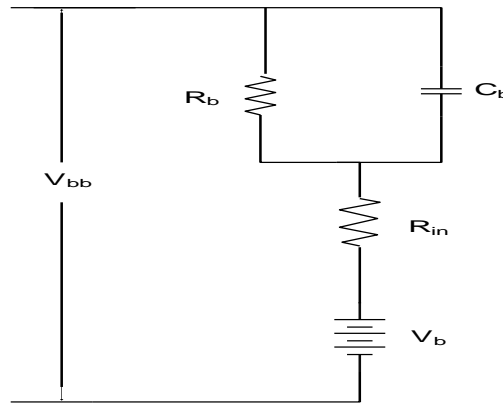


Fig 3.5 Circuit diagram of Battery energy storage system[2]

#### BESS nominal voltage

The minimum BESS nominal voltage is computed as

$$V_{bb} \geq \left( \frac{2\sqrt{2}}{\sqrt{3}} \right) V_L = 653 \text{ V} \quad (3.11)$$

Where  $V_L$  is the line voltage i.e. 400 v. hence  $V_{bb}$  is chosen as 756 v.

#### Parallel circuit capacitor and resistance

The capacitor value for the parallel circuit is computed as

$$C_b = \frac{kWh * 3600 * 1000}{0.5 \left( (V_{bbmax}^2) - (V_{bbmin}^2) \right)} \quad (3.12)$$

Where the minimum discharge battery voltage ( $V_{bbmin}$ ) of 661.5 V and maximum discharge battery voltage ( $V_{bbmax}$ ) of 850 V is used. Assuming the storage capacity of battery 110kWh to feed the rated consumer loads of 4.5 kW for 10 hours when the wind speed is low and generated power is negligible, the value of the battery capacitor is mathematically obtained as 9120 F. The value of  $R_b$  is considered as 10k ohm for self-discharging circuit.

### 3.3.2. Voltage source converter (VSC)

Voltage source converter is designed for 11.67kVA, 400 V, 4pole, 50 Hz, 0.9 lagging power factor PMSG-based SWECS to feed three phase three wire loads. The PMSG supplies rated power of 10.5 kW at rated voltage of 400 V when it is running at rated speed of 1500 rpm. The required rating of a Battery energy storage system and its voltage are chosen as per the mathematical formula mentioned above. The apparent rating of VSC is computed assuming the system is delivering generated power to rated three phase three wire loads at 0.8 lagging power factor as

$$S_{vdc} = \sqrt{P_L^2 + Q_L^2} \quad (3.13)$$

Where  $Q_L$  is the reactive power required by PMSG to regulate rated voltage under rated load conditions. The value of  $P_L$  and  $Q_L$  are taken as 6.4kW and 4.8kVAR. The value of  $V_{bb}$  is obtained as 756 V and the current rating of voltage source converter is calculated as

$$\sqrt{3}V_L I_{vsc} = 10 \text{ kVA} \quad (3.14)$$

The value of  $I_{vsc}$  is obtained as 14.43 amps.

### 3.3.3 Voltage frequency controller (VFC)

The VFC is implemented based on Synchronous reference theory (SRF) of control. In this method active component and reactive component of reference source current is computed as shown in Fig 3.6. The

tuning of pi controllers are done by hit and trail method. The reference voltage is taken as 320 V and reference frequency is taken as 48.2 Hz.

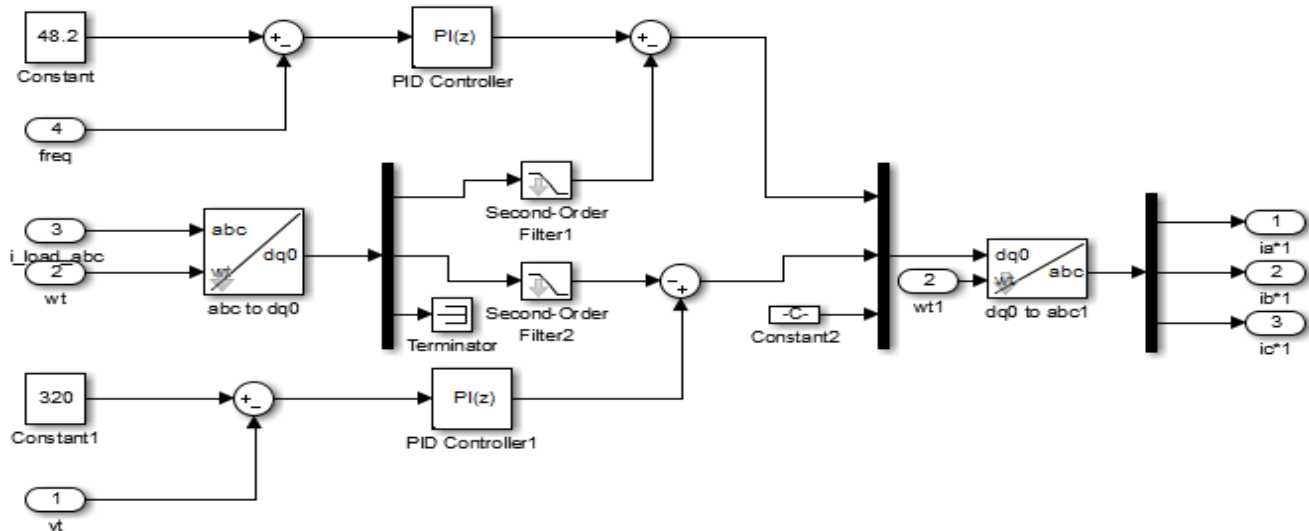


**Fig 3.6 Simulink model for SRF scheme based VF control**

### 3.3.4 Three phase three wire loads

The three phase loads are connected via circuit breakers as shown in Fig 3.7. Three phase fault is connected to the load to create a single phase and three phase fault during simulation. The second load which is initially open is used for over loading purpose which is connected via a circuit breaker to the system at a specified time. The circuit breakers are used for time specific opening and closing of loads to the WECS. The three phase fault is initially not connected. The transition time from open position to close position is mentioned in the Simulink block model of three phase fault.

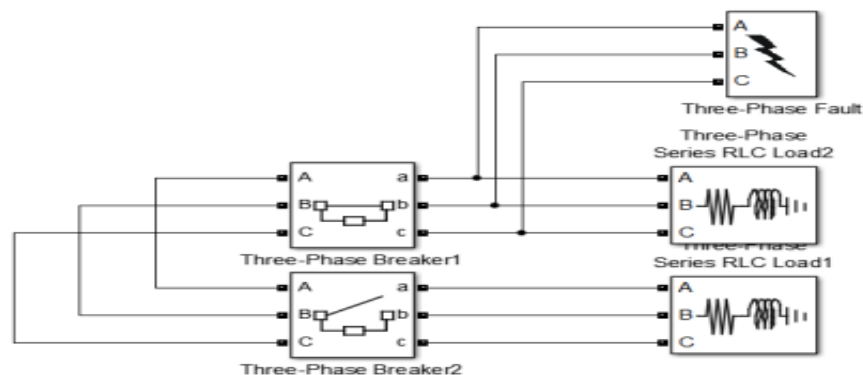


**Fig 3.7 Simulink model for three phase three wire loads and three phase fault using circuit breakers**

### 3.3.5 Interfacing inductors

The interfacing inductor between three phase output terminals of PMSG and the VSC is obtained as

$$L_i = \frac{\sqrt{3} * m * V_{bb}}{12 * a * f_s * i_{pp}} \quad (3.15)$$

Where modulation index (m) is considered as 1, overloading factor (a) is selected as 1.2,  $V_{bb}$  is taken as 756 V, peak to peak ripple current ( $i_{pp}$ ) through VSC equals 5% of the rated current (14.43 A) and switching frequency of VSC( $f_s$ ) equal to 3.14 kHz, the value of  $L_i$  is obtained as 50 mH.

### 3.3.6 Maximum current through IGBT

For considering 5% of peak to peak ripple current, the maximum current through an IGBT is obtained as

$$I_s = 1.25(i_{pp} + \sqrt{2}I_{vsc}) \quad (3.16)$$

This is obtained as 26.41 A. An IGBT of 26 A, and 1000 V rating is selected based on its availability.

### 3.3.7 Ripple filter

The ripple filter is the series combination of a resistance and a capacitance as shown in Fig 3.8. The filter is used to block the generated high frequencies and unwanted harmonics in the generated voltages. A low impedance of 5.92 ohm and capacitance of 10 $\mu$ F is selected for elimination of harmonics. The combination offers the total impedance of 319 ohm at fundamental voltage.

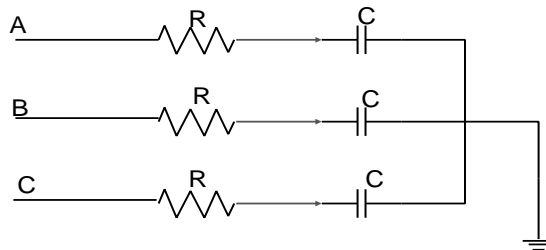


Fig 3.8 Ripple filter



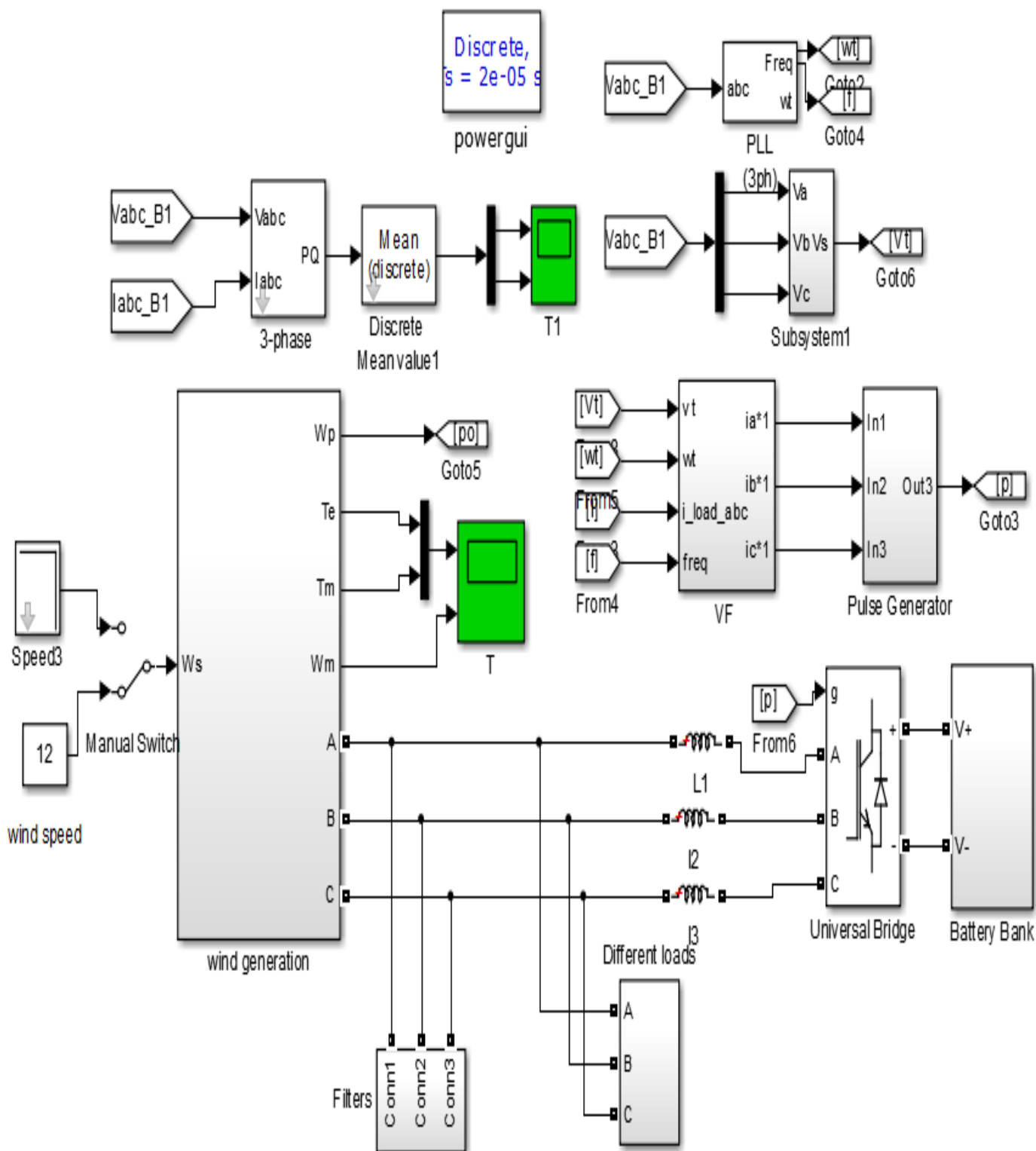
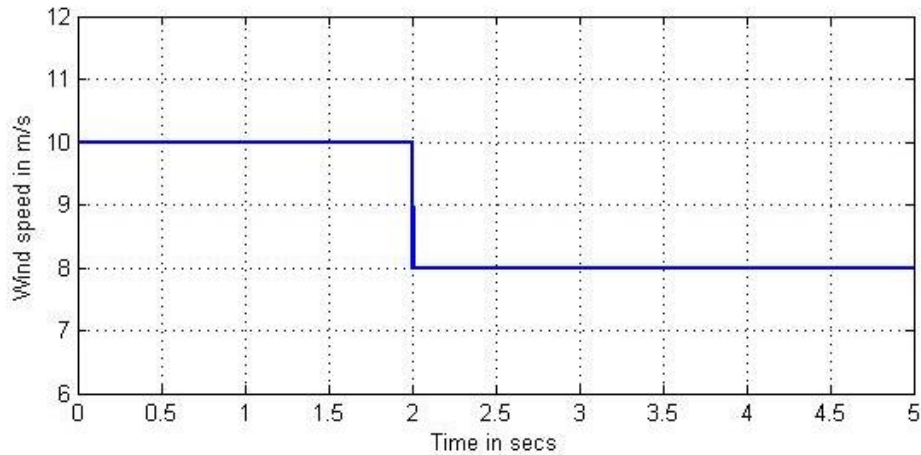


Fig 3.9 Simulink model of SWECS with VF controller

## 3.4 SIMULATION RESULTS

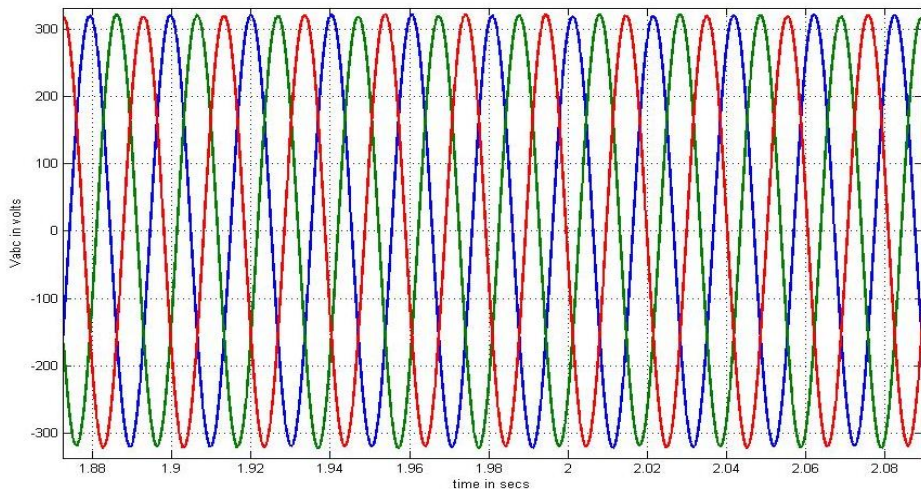
### 3.4.1 Simulation result for variable wind speed.

The wind speed is changed in a unit step manner. Initially the wind speed is 10 m/sec and after step change the wind speed is 8 m/sec as shown in Fig 3.10. The response of the VF controller is recorded against this step change in the following diagrams.



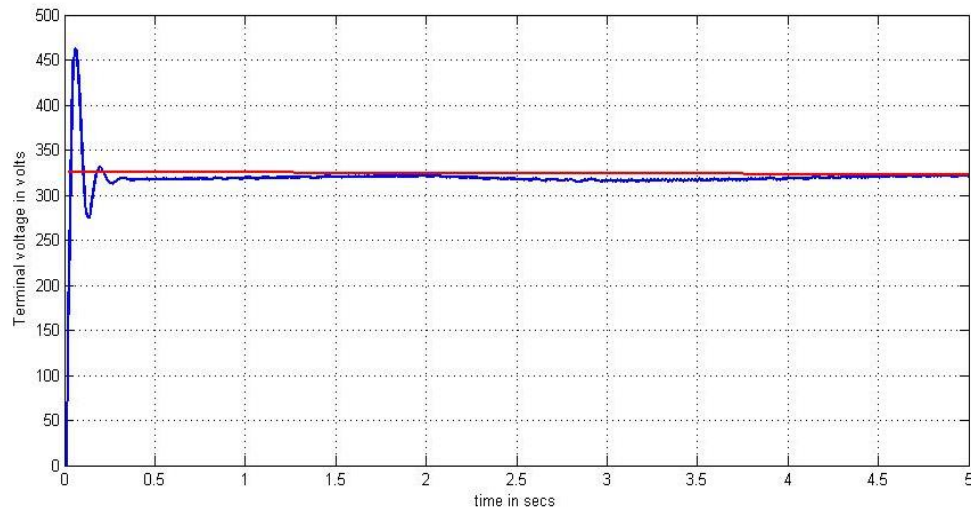
**Fig 3.10 Variable wind speed**

The three phase source voltage before change in wind speed is 320 V and after change in wind speed to 8m/sec the voltage remains almost around 320 V as shown in Fig 3.11. The imbalances seen in the diagram is due to controlling action of VF controller.



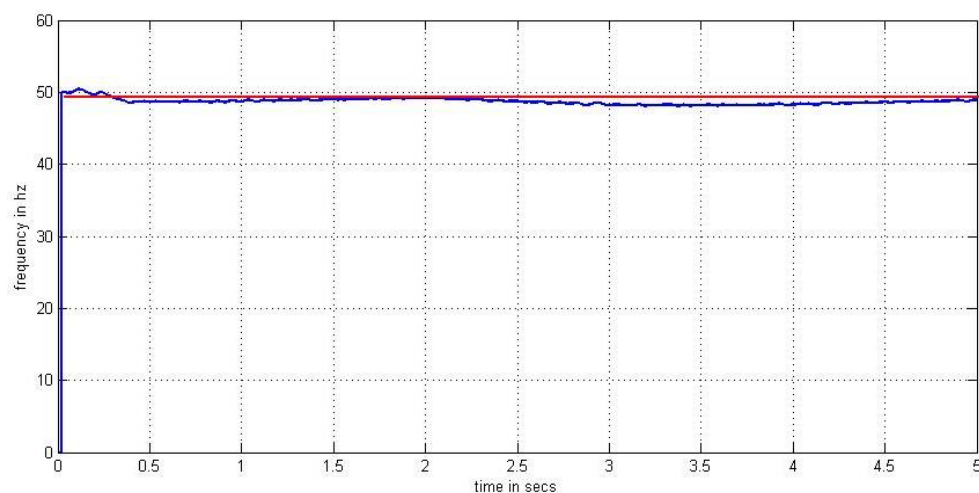
**Fig 3.11 Three phase generated voltage of PMSG**

The reference terminal voltage is taken as 320 V. Before change in wind speed the terminal voltage is around 325 V as shown in Fig 3.12. When the wind speed is changed to 8 m/sec, the terminal voltage still remains around 320 V. This shows the voltage is controlled in drastic change in wind speed.



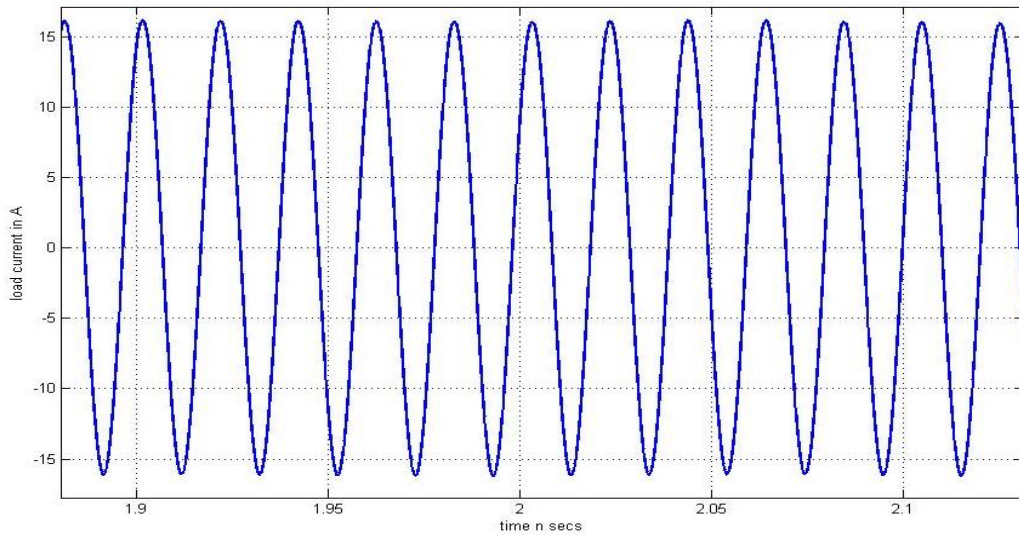
**Fig 3. 12 Terminal voltage of PMSG**

The system frequency is 50 Hz. When the wind speed is 8 m/sec, the system frequency is computed using a three phase PLL which gives frequency around 50 Hz as shown in Fig 3.13. When the wind speed changes to 8 m/sec, the system frequency varies very slightly and stays around 50 Hz. This shows that the frequency is controlled properly by the VF controller in drastic change in wind speed.



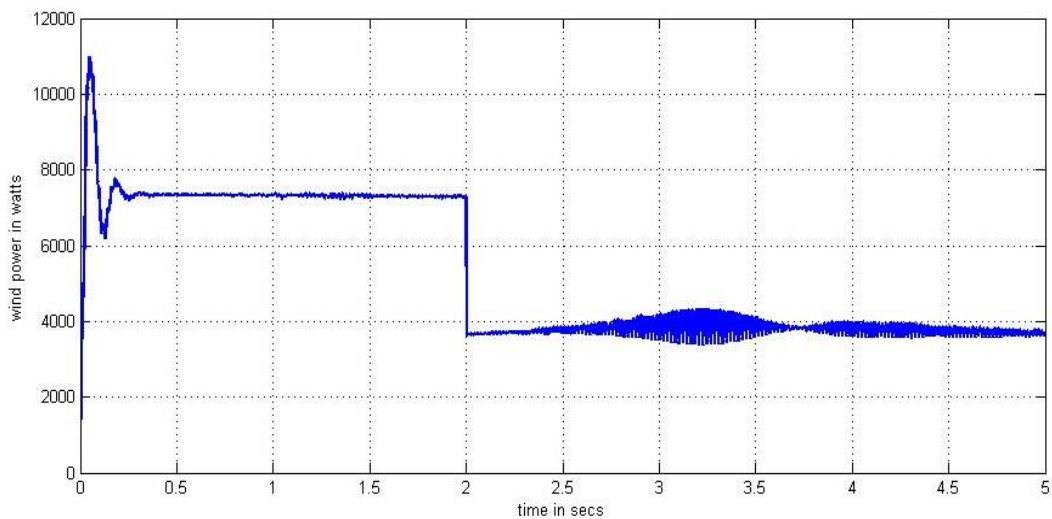
**Fig 3. 13 System frequency**

When the wind speed is 10 m/sec, the load current is around 16 A. When the wind speed is changed to 8 m/sec, due to VF controller the load current is maintained around 16 A as before the change in wind speed as shown in Fig 3.14.



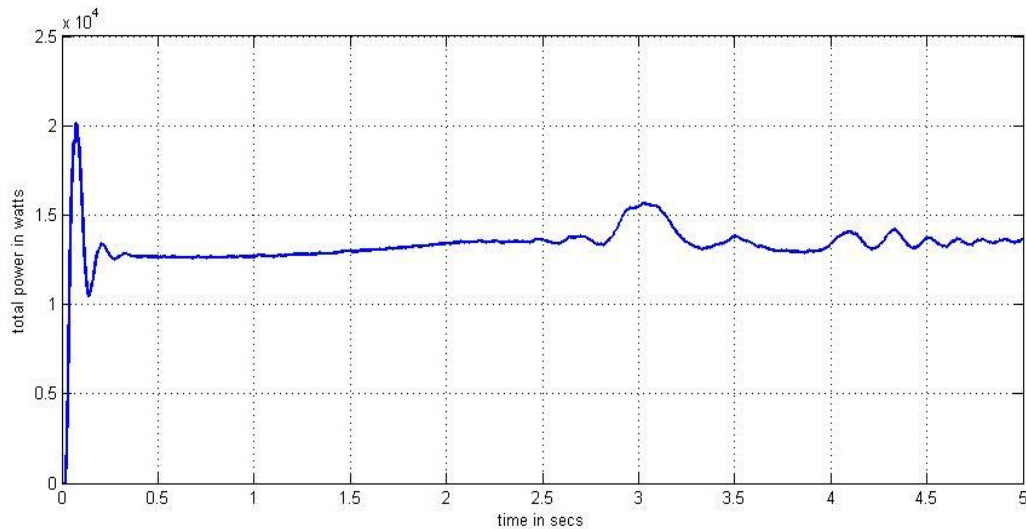
**Fig 3. 14 Load current**

The wind power when the wind speed is 10 m/sec is around 8 kW. When the wind speed decreased to 8 m/sec the wind power too decreased in a step down manner to 4 kW as shown in Fig 3.15.



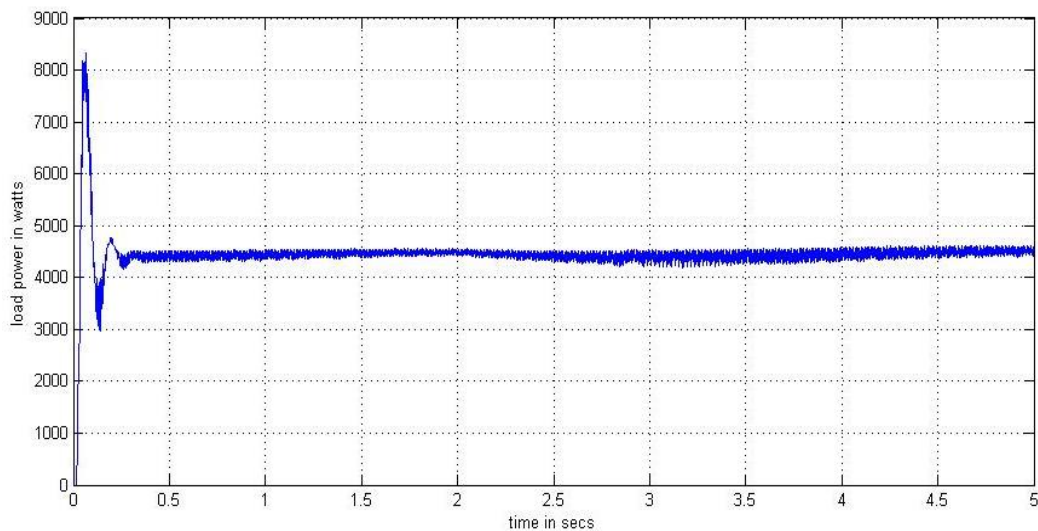
**Fig 3. 15 Power produced by wind turbine**

The generated power before change in wind speed was around 10.5 kW which is the rated power (Fig 3.16). After decrease in wind speed from 10 m/sec to 8 m/sec, the generated power is remained constant around 10.5 kW due to VF controller. This shows the working of VF controller in drastic change in wind speed.



**Fig 3.16 Generated power of PMSG**

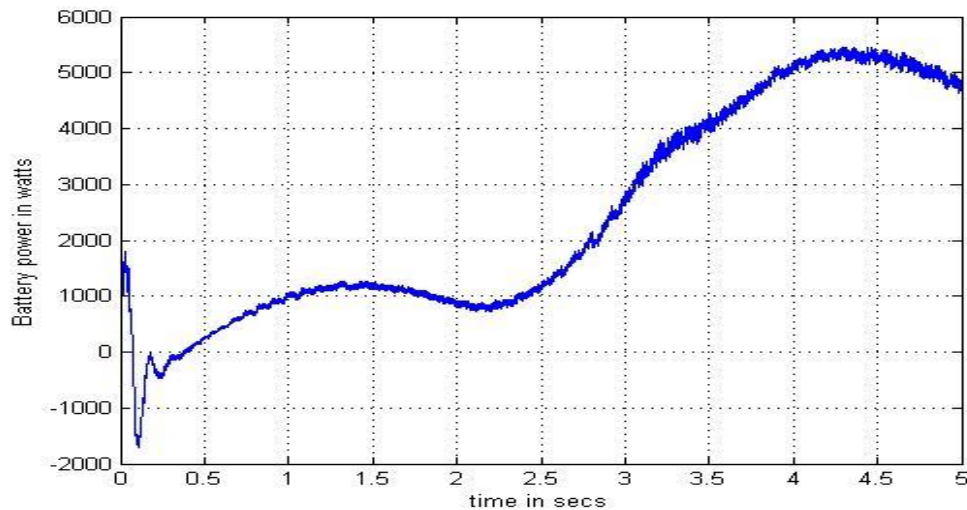
The load power before change in wind speed is around 4.5 kW and after change in wind speed is around 4.5 kW due to VF controlling action (Fig 3.17).



**Fig 3.17 Load power**

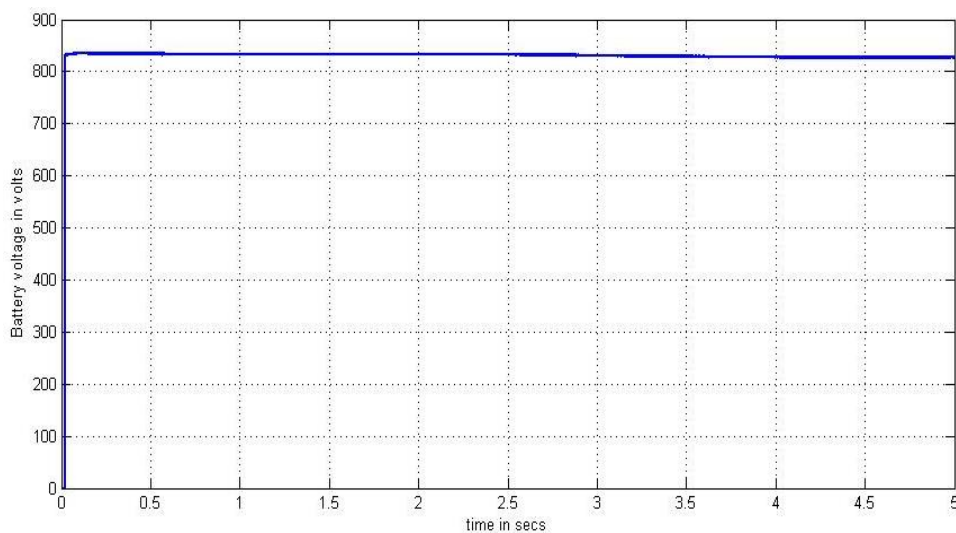


Before the change in wind speed, the battery power was around 1 kW and after deficiency in system power due to decrease in wind speed from 10 m/sec to 8 m/sec, the battery supplies the required power by increasing to 5 kW. Hence the BESS works according to the need of the SWECS under drastic change in wind speed. Fig 3.18 shows the battery energy storage system response to change in wind speed



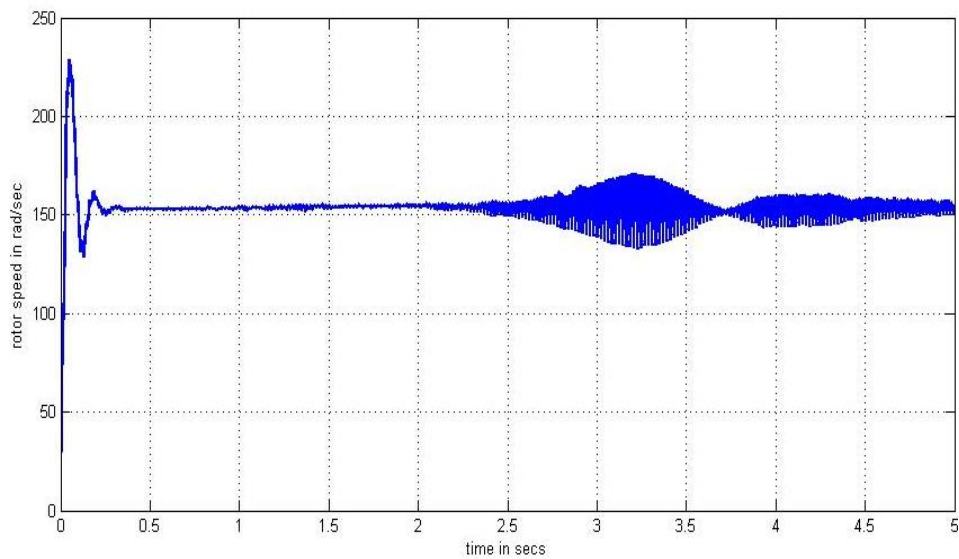
**Fig 3. 18 Battery power**

The battery voltage before change in wind speed is around 820 V and after change in wind speed, is around 820 V. Hence the battery voltage remains constant irrespective of change in wind speed as shown in Fig 3.19,.



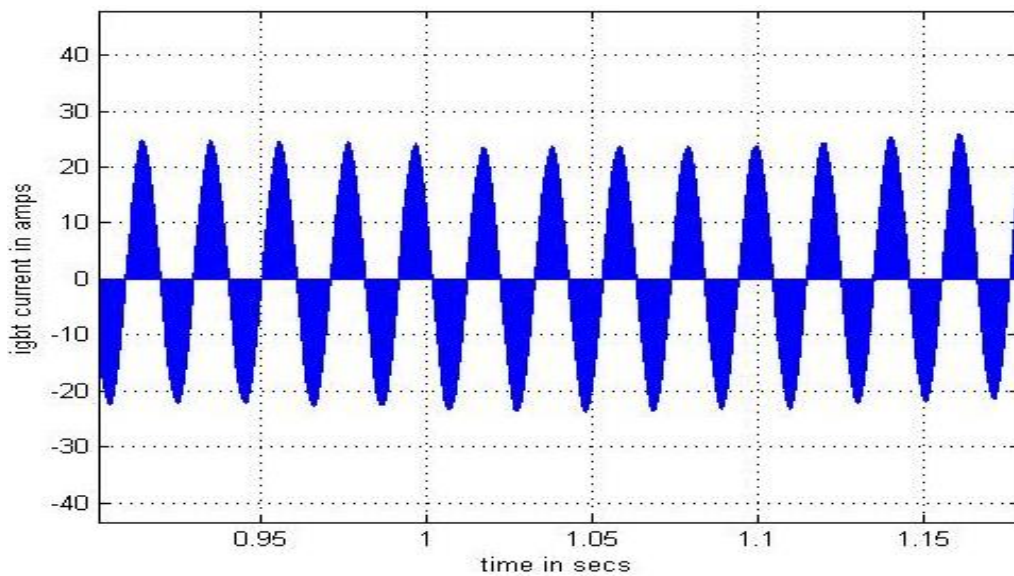
**Fig 3. 19 Battery terminal voltage**

The rotor speed before change in wind speed is around 152.8 rad/sec as shown in Fig 3.20. After wind speed changes, the rotor speed remains unchanged due to VF controlling action. The speed is still around 152 rad/sec.



**Fig 3.20 Rotor speed of PMSG**

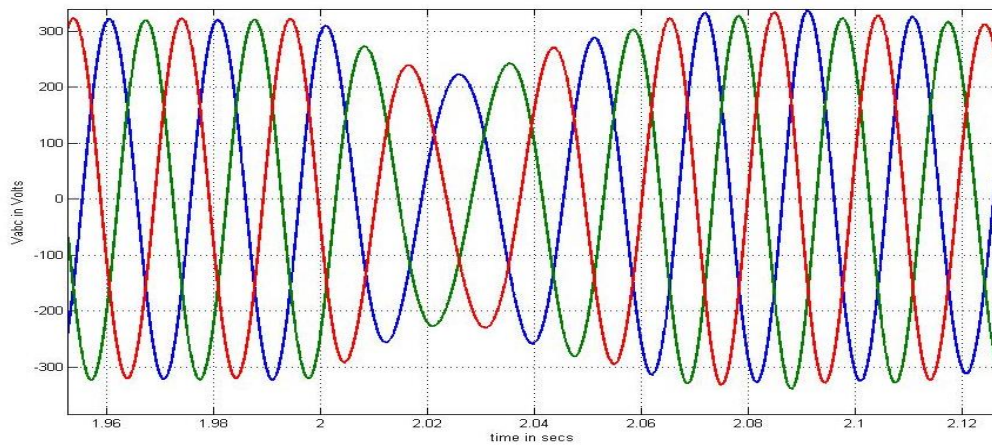
The maximum value of IGBT current is calculated as 27 A. From the Fig 3.21 below, it is very clear that the IGBT is operating under stress condition with IGBT current of 24 A.



**Fig 3.21 IGBT current**

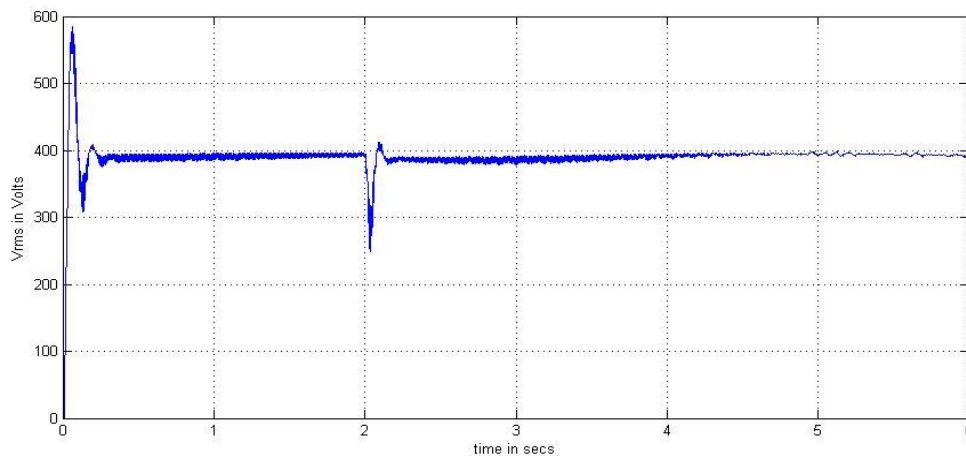
### 3.4.2 Simulation result for load change

Simulation is carried out for constant wind speed and increase in consumer load. The wind speed is kept constant at 10 m/sec. As shown in Fig 3.22, the generated voltage is around 320 V. The consumer load is kept constant around 4.5 kW. At  $t = 2$  secs, the consumer load is increased by connecting another three phase three wire load to the system via circuit breaker. The circuit breaker is controlled by mentioning the transition status and transition time. The total load becomes 9 kW. But the VF controller has able to maintain constant generated voltage with small variation at  $t = 2$  secs. The generated voltage is around 320 V.



**Fig 3.22 Generated three phase ac voltage of PMSG**

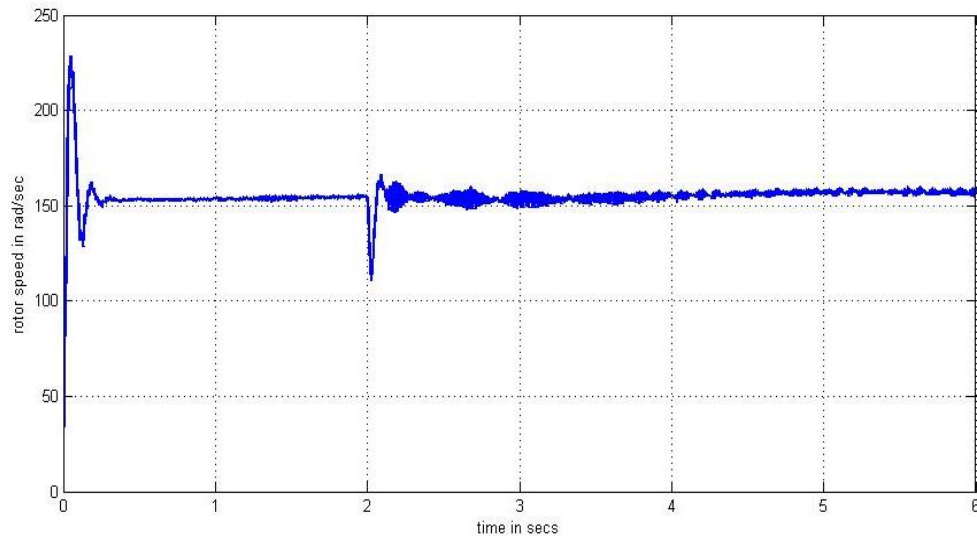
The RMS value of three phase ac generated voltage before change in consumer load is around 400 V as shown in Fig 3.23. After the consumer load increases, the RMS value remains constant at 400 V.



**Fig 3.23 RMS voltage of three phase ac generated voltage.**

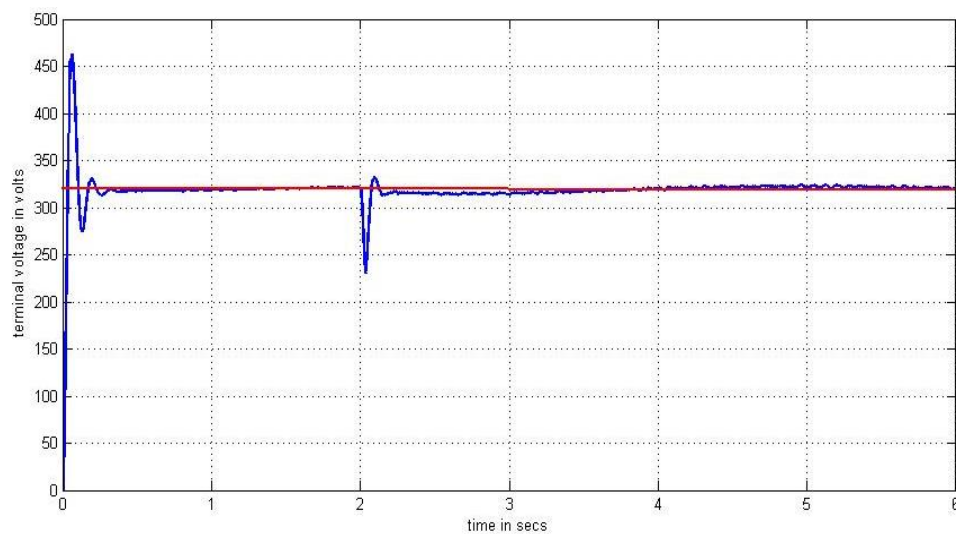


In Fig 3.24, the rotor speed at constant wind speed of 10 m/sec, is around 152.8 rad/sec. at  $t = 2$  secs, the consumer load increases from 4.5 kW to 9 kW, but due to VF controller the rotor speed is remained constant around 153 rad/sec with small variation at  $t = 2$  secs due to controlling action.



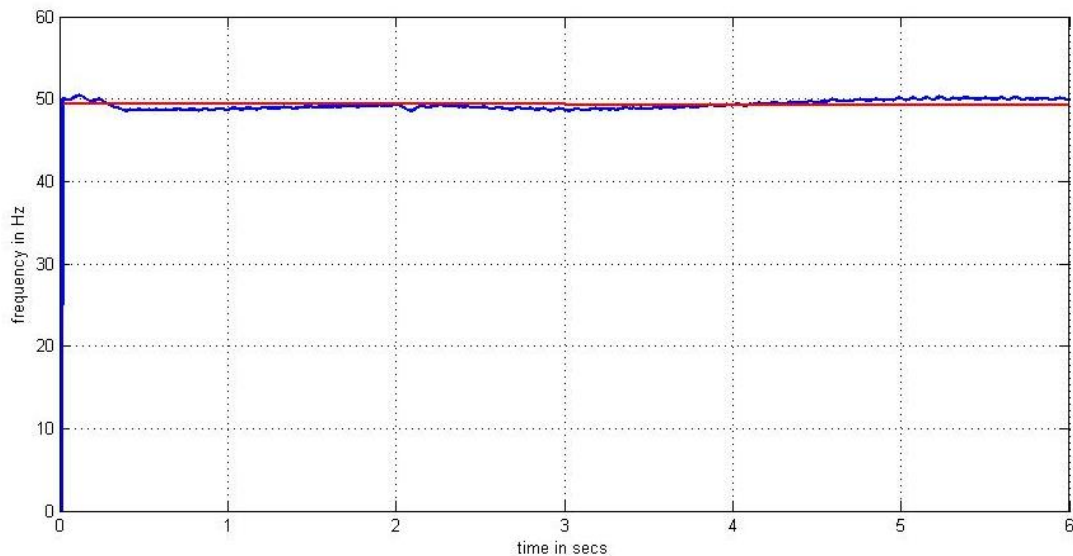
**Fig 3.24 Rotor speed of PMSG**

The terminal voltage is computed and compared with the reference value of 320 V. before change in consumer load, the terminal voltage is around 320 V as shown in Fig 3.25. At  $t = 2$  secs, the consumer load increases from 4.5 kW to 9 kW. The terminal voltage is remained constant due to controlling action of VF controller. The terminal voltage is around 320 V.



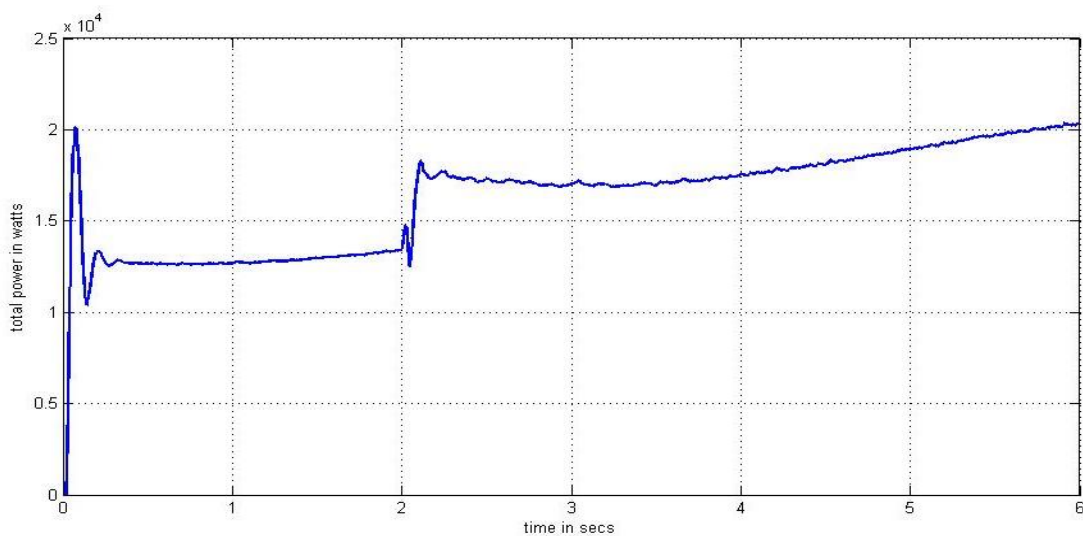
**Fig 3. 25 Terminal voltage of PMSG**

The system frequency is computed by using a three phase PLL and compared with the reference value of 50 Hz. Before change in consumer load, the system frequency is around 50 Hz as shown in Fig 3.26. At  $t=2$  secs, the consumer load increases keeping wind speed constant. But the frequency remains around 50 Hz due to controlling action of VF controller.



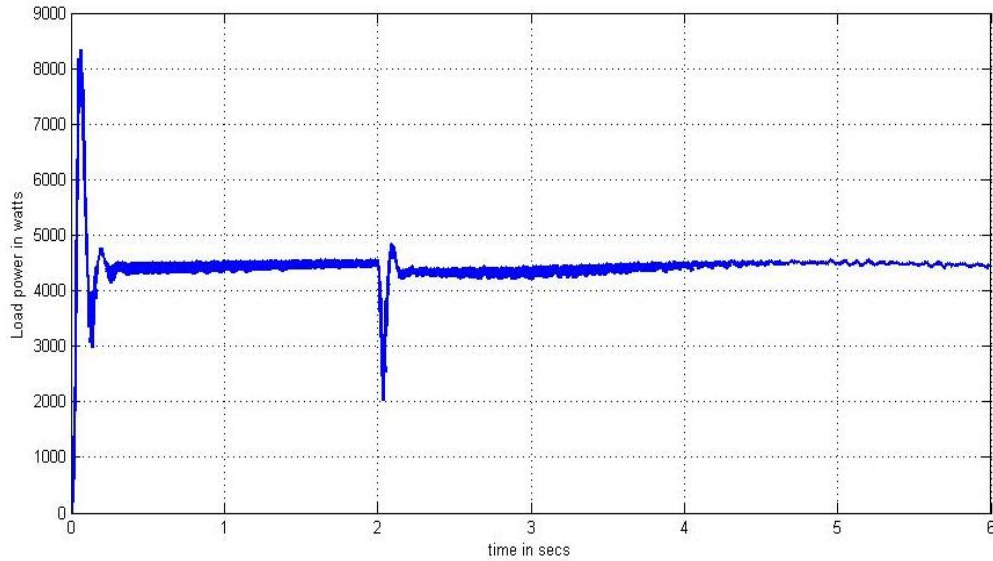
**Fig 3.26 System frequency**

The generated power at constant wind speed is around 10.5 kW. At  $t=2$  secs, the load power increases from 4.5 kW to 9 kW, hence the total generated power increases to 1.8 kW (Fig 3.27).



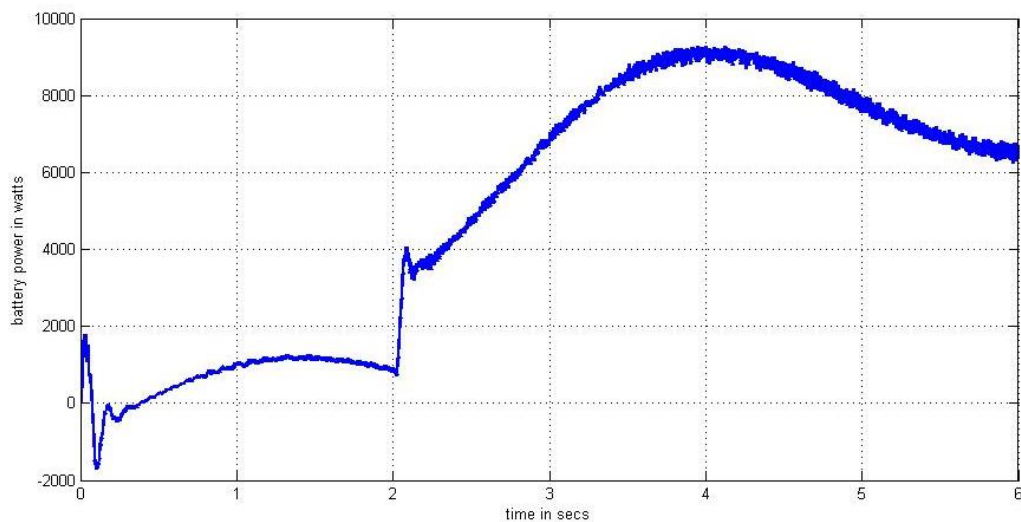
**Fig 3. 27 Generated power of PMSG**

At constant wind speed of 10 m/sec and constant consumer load of 4.5 kW, the load power remains constant around 4.5 kW as shown in Fig 3.28. At  $t = 2$  secs, the consumer load increases via circuit breaker. But the load power remains constant due to controlling action of VF controller. The variation at 2 sec is due to controlling action of VF controller.



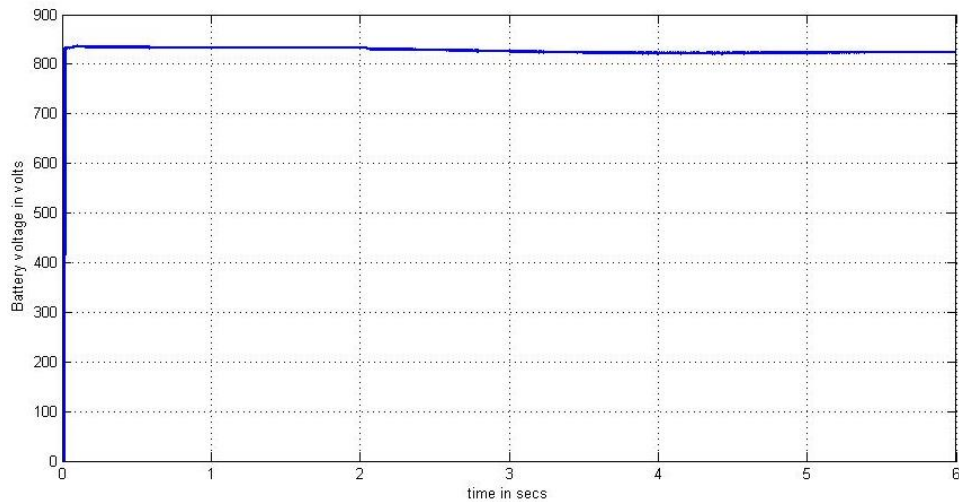
**Fig 3.28 Load power**

At constant wind speed of 10 m/sec and constant consumer load of 4.5 kW, the battery power remains almost constant around 1 kW as shown in Fig 3.29. At  $t = 2$  secs, the battery responds to the change in consumer load by supplying deficient power. After increase in load, the battery power increases to 7 kW.



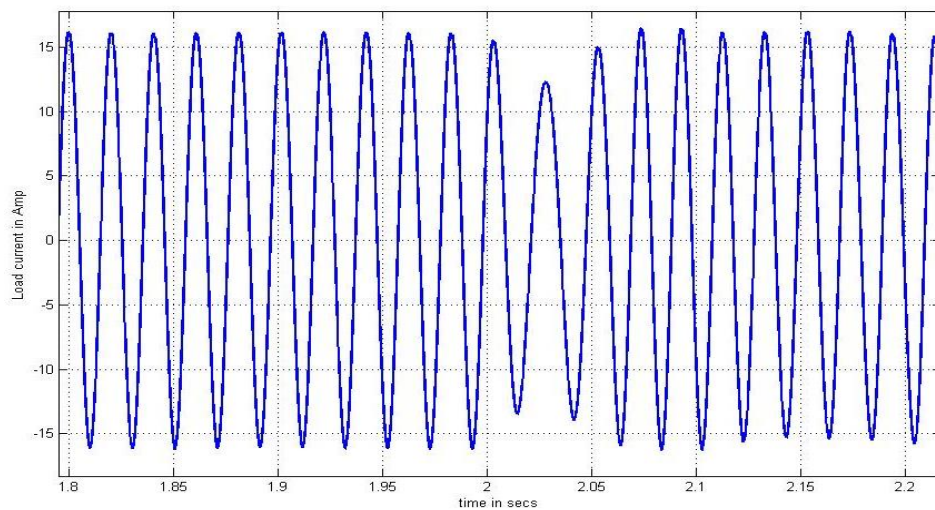
**Fig 3.29 Battery power**

The battery voltage before change in consumer load is around 820 V as shown in Fig 3.30. After increase in consumer load to 9 kW, due to VF controlling action the voltage remains constant around 820 V.



**Fig 3.30 Battery terminal voltage**

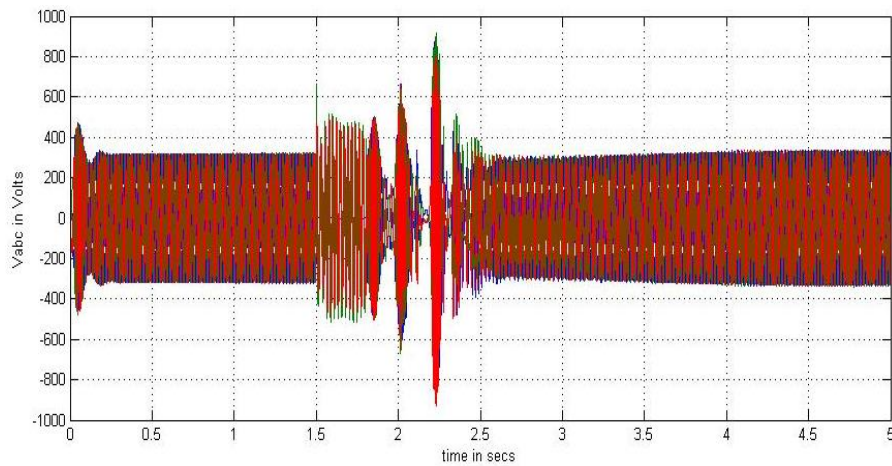
The load current before change in consumer load is around 15 A as shown in Fig 3.31. after consumer load is increased at  $t = 2$  secs, the load current decreases for few milli secs and finally restores to original value of around 15 A.



**Fig 3.31 Load current**

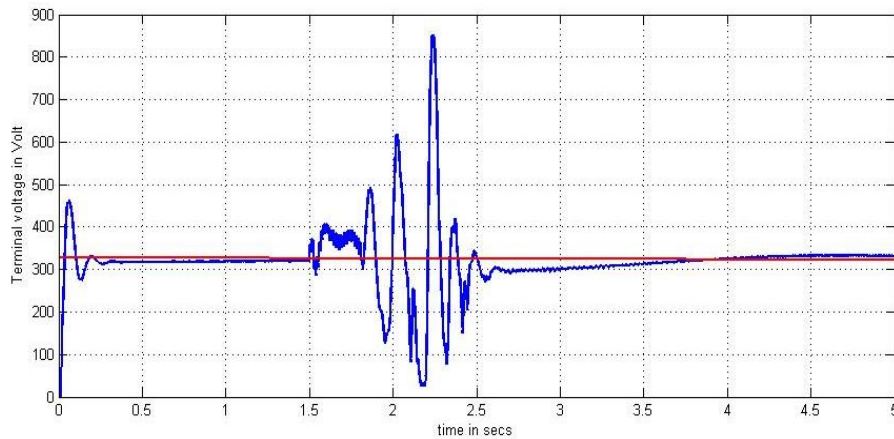
### 3.4.3 Simulation for Fault current occurrence at line

The simulation of WECS is performed under constant wind speed, constant consumer load and fault occurrence at load terminals. The wind speed is 10 m/sec, consumer load is 4.5 kW and the generated three phase ac voltage is around 320 V (Fig 3.32). At  $t = 1.5$  sec, single phase fault is applied by disconnecting phase A of the load terminals. Due to controlling action of VF controller, the system is able to maintain its generated three phase ac voltage around 330 V. the distortion at  $t = 1.5$  to  $t = 2$  secs is due to controlling action of the controller.



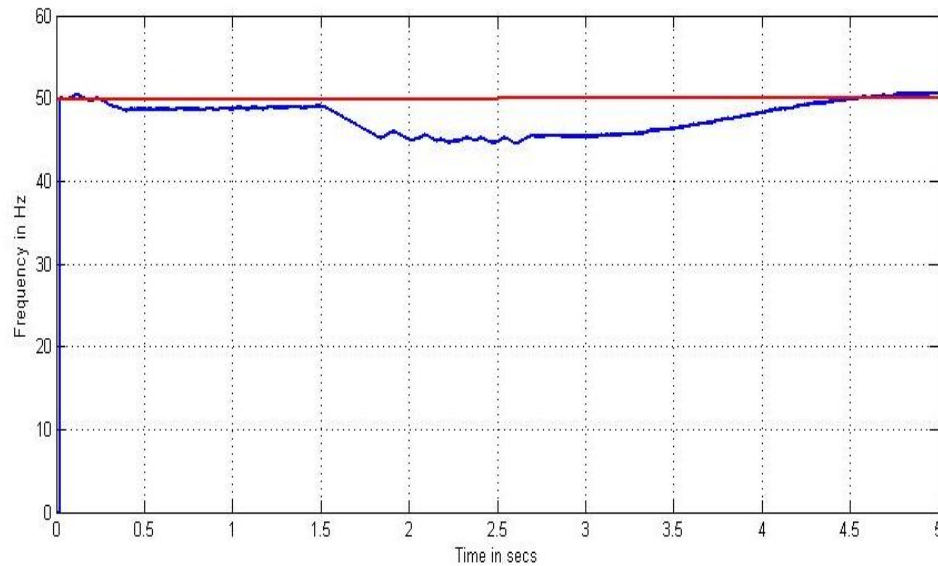
**Fig 3.32 Three phase ac generated voltage of PMSG**

The terminal voltage before fault occurrence is around 320 V (Fig 3.33). At  $t = 1.5$  sec, single phasing of load terminal is done. The terminal is maintained constant around 320 V due to controlling action of VF controller.



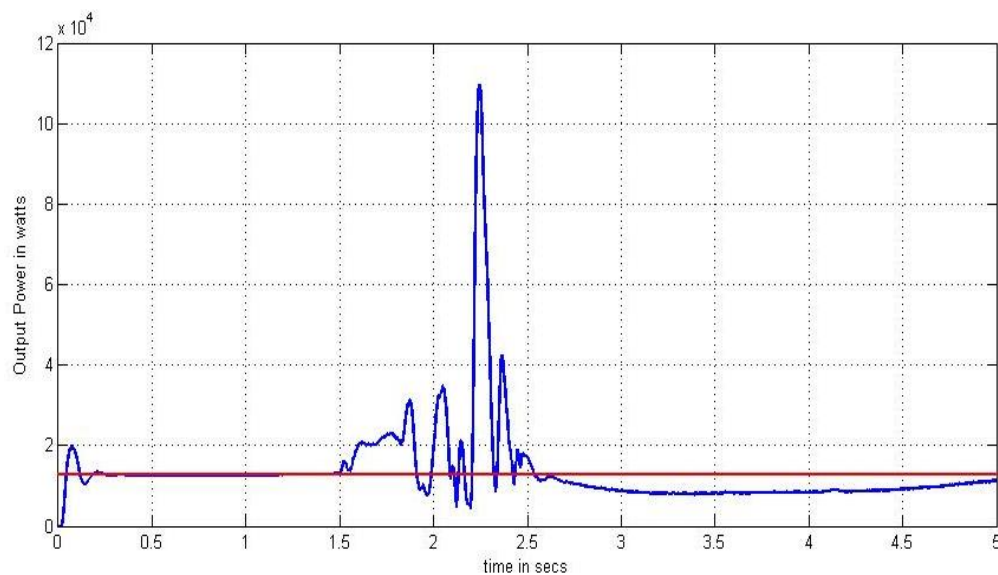
**Fig 3. 33 Terminal voltage of PMSG**

The system frequency before fault occurrence is around 50 Hz. At  $t = 1.5$  sec, the VF controller is able to maintain the system frequency around 50 Hz as shown in Fig 3.34..



**Fig 3.34 System frequency**

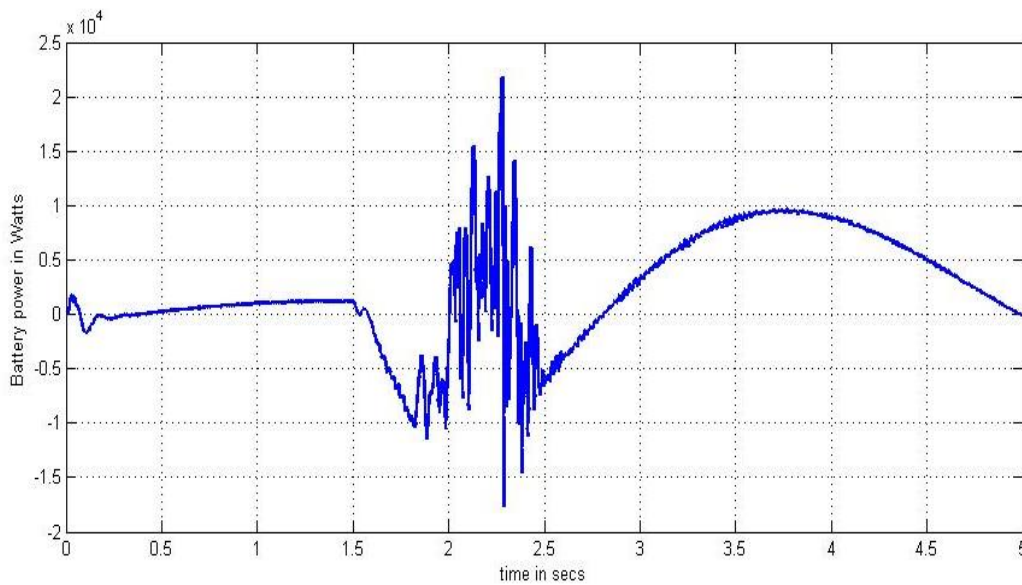
The output generated power before fault occurrence is around 10.5 kW (Fig 3.35). At  $t = 1.5$  sec, single phasing of load terminal is done. Due to VF controlling action the generated power is maintained constant around 11 kW.



**Fig 3.35 Total generated power of PMSG**

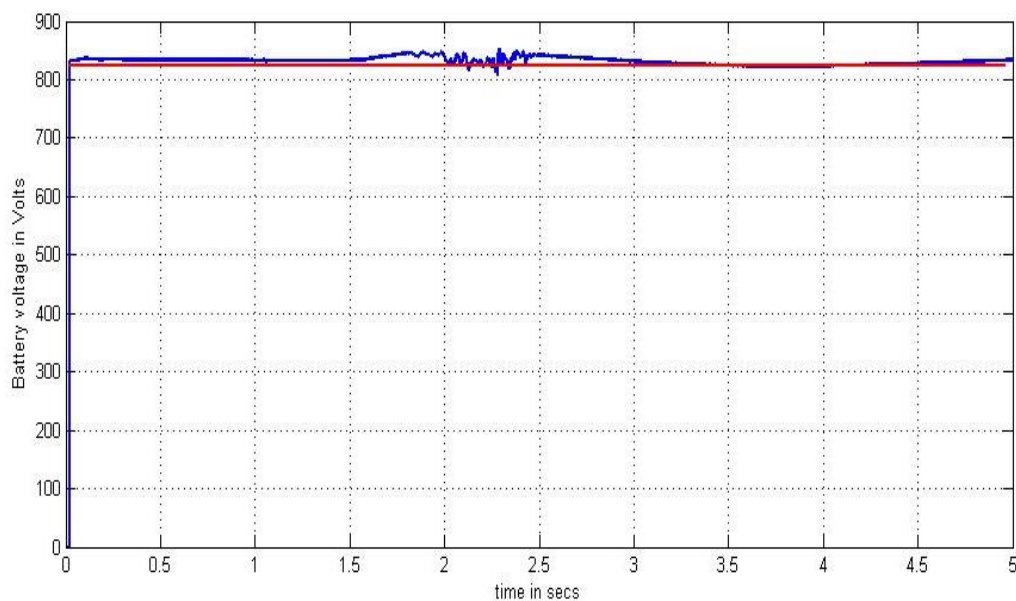


Fig 3.36 shows battery power before fault occurrence. The battery power is around 1 kW. At  $t = 1.5$  sec the battery responds by supplying deficient power. The average battery power is around 0.5 kW.



**Fig 3. 36 Battery power**

Fig 3.37 shows battery voltage at constant wind speed and constant consumer load is around 820 V. at  $t = 1.5$  sec, the battery voltage remains constant around 820 V due to controlling action of VF controller.



**Fig 3. 37 Battery terminal voltage**

## CHAPTER 4

### CONCLUSION

The PMSG based WECS was modeled and simulated using MATLAB & SIMULINK. The P&O MPPT control technique was implemented using a boost converter. Wind speed was varied in a step up manner from 8 m/sec to 10 m/sec and response of the controller is recorded. The plots of generated output power, dc link voltage, and output three phase voltage was recorded. The proposed model is run for 5 sec first without MPPT control and then with MPPT control. The power generated without MPPT controller was low i.e. 4.5 kW and the power generated with a MPPT controller is around 6 kW. This shows the improvement in the conversion efficiency of the controller. Most of the power loss occurs in VSC switches and converters. Hence the proposed MPPT method is utilized and it is seen that the efficiency of power conversion is increased to around 40%. The SWECS was tested against step change in wind speed from 10 m/s to 8m/s at  $t = 2$ secs, change in load from normal loading to over loading and three phase fault at line. First the SWECS was run without VF controller against above conditions and the results were noted down. It is seen from the figures that during change in wind speed at  $t = 2$ secs the power extracted from the wind decreases, three phase generated voltage from PMSG decreases, terminal voltage decreases, frequency fluctuation occurs, load power decreases, active power of the system decreases. Hence the system has under-performed. This kind of performance is also expected during over loading condition and three phase fault condition at line. Therefore the efficiency of the SWECS is way below normal value. The simulation was then run with SWECS connected to VF controller, VSC and BESS against mentioned conditions. It was observed that during change in wind speed, over loading and single phase fault the system is able to maintain its terminal voltage, system frequency around 50 Hz, constant load power, balanced three phase generated voltage, rated rotor speed. The battery provided the required power during deficient in power and over loading conditions BESS has been used in all condition for load leveling. With the demonstrated performance, it have been shown that devised VFCs performs satisfactorily as a load leveler, a load balancer, a phase balancer under change in wind speed and consumer load



## **SCOPE OF FUTURE WORK**

1. Development of hybrid wind and solar energy conversion system for maximum utilization of renewable energy sources
2. Implementation of SWECS with nonlinear and dynamic loads
3. Development of more efficient maximum power tracking method based on variable step size and variable pitch angle of wind turbine
4. Connection of stand-alone wind energy conversion system to a micro grid.
5. Development of more efficient voltage frequency controller in order to reduce harmonics and produce low switching losses.
6. Hardware implementation of WECS with VF controller connected to three phase four wire loads

## REFERENCE

- [1] Hyeung-Gyun Kim, Dong-Choon Lee, Jul-Ki Seok, and G-Myoung Lee, "Stand-alone wind power generation system using vector-controlled cage-type induction generators," in *Proc. of Inter. Conference on Electrical Machines and systems*, vol.1, pp.289-292, Nov.2003.
- [2] Bhim Singh and Gaurav Kumar Kasal, "Voltage and Frequency Controller for a three-phase four wire autonomous wind energy conversion systems," *IEEE Trans. Energy Conversion*, vol. 23, no.2, pp.509–518, June 2008.
- [3] S.Grabic, N. Celanovic and V.A Katic, "Permanent Magnet Synchronous Generator Cascade for Wind Turbine Application," *IEEE Trans. On Power Electronics*, vol. 23, no. 3, pp.1136 – 1142, May 2008.
- [4] F.Valenciaga and M.R. Puleston, "High-Order Sliding Control for a Wind Energy Conversion System Based on a Permanent Magnet Synchronous Generator," *IEEE Trans. on Energy Conversion*, vol.23, no.3, pp. 860-867, Sept. 2008.
- [5] M.Popesci, M.V. Cistelecan, L.Melcescu, and M. Covrig, "Low Speed Directly Driven Permanent Magnet Synchronous Generators for Wind Energy Applications," in *Proc. Of International Conf. on Clean Electrical Power*, 2007. ICCEP '07, pp:784 – 788, 21-23 May 2007.
- [6] M.Chinchilla, S.Arnaltes, and J.C.Burgos, "Control of permanent magnet generators applied to variable-speed wind-energy systems connected to the grid", *IEEE Trans. on Energy Conversion*, vol. 21, no.1, pp.130 – 135, March 2006.
- [7] C.V Nayar, J. Perihia, F. Thomas, S,J.Philips, T.Pryor and W.L.James, "Investigation of Capacitor excited induction generators and permanent magnet alternators for small scale wind power generation " *Renewable Energy*, vol.1, no.3/4, pp.381–388, July 1991.
- [8] B S .Borowy and Z M Salameh, "Dynamic response of a stand-alone wind energy conversion system with battery energy storage to a wind gust," *IEEE Trans. on Energy Conversion*, vol.12, no.1, Mar. 1997.
- [9] Hurng-Liahng, Kuen- Der Wu, Jinn- Chang Wu and Wen- Jung Chiang, "A three-phase four- wire power filter comprising a three-phase threewire active filter and a zig-zag transformer," *IEEE Trans. of Power Electronics*, vol. 23, no. 1, pp. 252- 259, January 2008.
- [10] S. Bhattacharya and D. Diwan, "Synchronous Frame Based Controller Implementation for a Hybrid Series Active Filter System", in *Proc. Of IEEE IAS Meeting*, pp 2531-2540, Jan 1995,.
- [11] Z.M.Salameh, M.A.Casacca and W.A. Lynch, "A mathematical model of lead acid batteries," *IEEE Trans. on Energy Conversion*, vol.7, no.1, pp. 93-97, Mar. 1992.

- [12] L.M.Fernandez, J.R.Saenz and F.Jurado, “dynamic Models of wind farms with fixed speed wind turbines,” *Renewable Energy*, vol.31, no.8, pp.1203–1230, July 2006.
- [13] Hurng- Liahng Jou, Kuen- Der Wu, Jinn- Chang Wu and Wen- Jung Chiang, “A three-phase four-wire power filter comprising a three-phase three-wire active filter and a zig-zag transformer,” *IEEE Trans. Power Electron.*, vol. 23, No. 1, pp. 252- 259, January 2008.
- [14] M.C. Benhabib and S. Saadate, “New control approach for four-wire active power filter based on the use of synchronous reference frame,” *Electric Power Systems Research*, vol. 73,no. 3, pp. 353-362, Mar 2005.
- [15] María Isabel Milanés, Enrique Romero Cadaval and Fermín Barrero González, “Comparison of Control Strategies for Shunt Active Power Filters in Three-Phase Four-Wire Systems,” *IEEE Transactions on Power Electronics*, vol. 22, no. 1, pp.229-236, Jan. 2007.
- [16] B S .Borowy and Z M Salameh, “Dynamic response of a standalone wind energy conversion system with battery energy storage to a wind gust,” *IEEE Trans. on Energy Conversion*, vol.12, no.1, Mar. 1997.